

SOLITARY WAVES AND HOMOCLINIC ORBITS

N. J. Balmforth

Institute for Fusion Studies, University of Texas, Austin, Texas 78712

KEY WORDS: chaos, pattern theory, nonlinear dynamics

1. SOLITARY WAVES IN FLUIDS

Ever since Russell's historic observation of a solitary wave in a canal, the notion that fluid motion often organizes itself into coherent structures has increasingly permeated modern fluid dynamics. Such localized objects appear in laminar flows and persist in turbulent states—from the water on windows on rainy days, to the circulations in planetary atmospheres.

This review concerns solitary waves in fluids. More specifically, it centers around the mathematical description of solitary waves in a single spatial dimension. Moreover, it concentrates on strongly dissipative dynamics, rather than integrable systems like the KdV equation. This divorces it from the theory of solitons, which develops analytically around the inverse scattering transform (e.g. Ablowitz & Segur 1981).

One-dimensional solitary waves, or *pulses* and *fronts* (*kinks*) as they are also called, are the simplest kinds of coherent structure (at least from a geometrical point of view). Nevertheless, their dynamics can be rich and complicated. In some circumstances this leads to the formation of spatio-temporal complexity in the systems giving birth to the solitary waves, and understanding such complexity is one of the major goals of the theory outlined in this review. Unfortunately, such a goal is far from achieved to date, and we assess its current status and incompleteness.

As experimental analogues of the pulse or frontal dynamics we explore, one can draw on recent experiments with real fluids. Closest to what we describe (in the sense that the equations we use as illustration were once

derived as a relevant model) are experiments on falling fluid films. There, as one can often observe on rainy windows and in gutters, waves moving down an incline steepen into propagating pulses (Alekseenko et al 1985, Liu et al 1993). Eventually they are deformed in a second dimension by secondary instabilities, but for a substantial fraction of their evolution, the fluid generates an essentially one-dimensional pulse train. Properties of such patterns of propagating pulses are reviewed by Chang (1994).

Another experimental scenario in which pulses are created involves the convection of a binary fluid (Anderson & Behringer 1990, Bensimon et al 1990, Moses et al 1987, Niemela et al 1990). When enclosed in a slender geometry like a thin annulus, this fluid can convect heat within localized packets of traveling cells. The manner in which such convective pulses drift, interact, and generally evolve provides a powerful visualization of pulse dynamics (Kolodner 1991a,b). Analogous states of excitation exist in liquid crystals (Joets & Ribotta 1988) and in fluids subject to Faraday instability (Wu et al 1984). Various other kinds of solitary waves in interfacial experiments are reviewed by Flesselles et al (1991).

In Section 2, we give a brief account of why, theoretically, we might expect many systems to generate solitary waves; we derive the complex Ginzburg-Landau equation for a spatially extended system near a Hopf bifurcation. The solutions of this equation suggest that one of the ramifications of overstability is frequently pulse and front generation. In Sections 3 and 4, we turn to the heart of the review: a discussion of the theory of solitary-wave equilibria and dynamics within a framework of asymptotic analysis and dynamical systems theory. In the final section we tie up some loose ends and briefly mention the standing of the theory with regard to real physical situations.

2. PRELIMINARIES: THE COMPLEX GINZBURG-LANDAU EQUATION

As a convenient example we take the partial differential equation (PDE)

$$\partial_t u + u \partial_x u + \partial_x^2 u + \mu \partial_x^3 u + \partial_x^4 u + \alpha u = 0, \quad (2.1)$$

where μ and α are parameters. This model equation, for $\alpha = 0$, was derived by Benney (1966) to describe instabilities on falling fluid films; u is the surface displacement about the uniformly thick state. Over a wide range in values of the parameters, this equation possesses solutions that take the form of patterns of pulses (Kawahara & Toh 1987; Elphick et al 1991a; Chang et al 1993a,b).

2.1 Hopf Bifurcation in an Extended System

The solitary structures observed in systems like binary-fluid convection in annuli occur near the Hopf bifurcation of a spatially extended (one-dimensional) system. In this circumstance, the equations governing the fluid can be asymptotically reduced to a complex Ginzburg-Landau equation governing the spatio-temporal evolution of the envelope of a wave (e.g. Manneville 1990). The thin-film equation (2.1) admits a spatially uniform equilibrium solution, $u = 0$, which undergoes such a bifurcation when we continuously vary α through positive values. Hence it provides a simple illustration of the derivation of the complex Ginzburg-Landau equation.

The bifurcation to instability occurs as α is decreased through $1/4$. Infinitesimal perturbations about this state have the dependence $\exp[i(kx + \omega t) + \eta t]$, where

$$\omega = \mu k^3 \quad \text{and} \quad \eta = 1/4 - \alpha - (k^2 - 1/2)^2. \tag{2.2}$$

Just below the critical point $\alpha_c = 0.25$, a band of wavenumbers surrounding $k = k_c = 1/\sqrt{2}$ becomes marginally unstable. Here, we set $\alpha = 0.25 - \varepsilon^2 \alpha_2$, where ε is a small parameter (quantifying “just below”) and α_2 is order unity. Near the maximally unstable wavenumber k_c , the dispersion relation reduces to

$$\omega \simeq \omega_c + \frac{3}{2} \varepsilon \mu K \quad \text{and} \quad \eta \simeq \varepsilon^2 (\alpha_2 - K^2), \tag{2.3}$$

where $\omega_c = \mu/2 \sqrt{2}$ and $k - k_c = \varepsilon K$.

In a spatially extended domain, we see that a packet of linearly unstable waves develops through instability over a distance of order ε^{-1} , and on a timescale of order ε^{-2} . Frequency corrections occur on the shorter time-scale ε^{-1} , however, and their dependence on K implies a drift in the envelope of the wave pattern, or a group velocity, εc_g , with $c_g = 3\mu/2$. This observation motivates our asymptotic scaling of Equation (2.1) in developing a weakly nonlinear theory for the evolution of the envelope of a wave pattern at finite amplitude. In particular, we seek a solution

$$u \sim \varepsilon [A(\varepsilon x, \varepsilon t, \varepsilon^2 t) e^{i(k_c x + \omega_c t)} + A^*(\varepsilon x, \varepsilon t, \varepsilon^2 t) e^{-i(k_c x + \omega_c t)}], \tag{2.4}$$

where $*$ means complex conjugate.

We now introduce the stretched timescales, $\tau = \varepsilon t$ and $T = \varepsilon^2 t$, and the long length scale, $X = \varepsilon x$, so the temporal and spatial derivatives become $\partial_t \rightarrow \partial_t + \varepsilon \partial_\tau + \varepsilon^2 \partial_T$ and $\partial_x \rightarrow \partial_x + \varepsilon \partial_X$. We further pose the asymptotic expansion

$$u = \varepsilon u_1 + \varepsilon^2 u_2 + \varepsilon^3 u_3 + \dots \tag{2.5}$$

of which the first term is given by the right-hand side of Equation (2.4). At subsequent orders we derive equations for u_2 , u_3 , and so on. As is typical in asymptotic expansions of this kind (Manneville 1990), these relations take the form of inhomogeneous linear equations. Requiring the corrections to be bounded enforces certain solvability conditions. In the example at hand, the first condition is

$$\partial_\tau A + c_g \partial_X A = 0, \quad (2.6)$$

which has solution $A = A(X - c_g \tau, T)$; as advertised, the envelope of the wave pattern moves with the group velocity c_g . A modulation equation for A actually emerges from solvability at order ϵ^3 . It is

$$\hat{g}_T A = \alpha_2 A + (4 - 3i\mu\sqrt{2})\partial_X^2 A - \frac{(10 + 7i\mu\sqrt{2})}{(50 + 49\mu^2)} |A|^2 A, \quad (2.7)$$

which is a particular case of the complex Ginzburg-Landau equation.

In this illustrative problem, the sign of the nonlinear term ensures that spatially homogeneous patterns emerge from equilibrium beyond a supercritical bifurcation. In other systems, the bifurcation of such patterns may be subcritical, as it is, for example, in binary fluid convection (Thual & Fauve 1988). In these cases the equation requires further regularization of some kind if the amplitude is not to grow without bound.

2.2 Real Ginzburg-Landau Equations

The complex Ginzburg-Landau equation simplifies substantially if all of the coefficients are real (so $\mu = 0$). After suitably rescaling, we then have

$$\partial_\tau a = \partial_X^2 a + (\alpha_2 - a^2)a, \quad (2.8)$$

where a is the real part of A . This real Ginzburg-Landau equation has been extensively studied in problems of phase separation in condensed matter physics. It has the spatially homogeneous solutions, $a = 0$ and $a = \pm\sqrt{\alpha_2}$. For $\alpha_2 > 0$, the equilibrium $a = 0$ is unstable, but the finite amplitude states are stable.

The real Ginzburg-Landau equation is of interest because it possesses solutions that take the form of fronts or kinks connecting the various homogeneous phases. The zero-amplitude equilibrium, for example, rapidly evaporates when the system generates fronts that advance through the domain, transforming the state to one of the stable phases (e.g. Ben-Jacob et al 1985, van Saarloos 1989). An example of one of these fronts is

shown in Figure 1*a*. Of more interest are the stationary kink solutions, $a = K(X)$, that connect the two stable phases:

$$K(X) = \sqrt{\alpha_2} \tanh(X\sqrt{\alpha_2/2}) \tag{2.9}$$

(see Figure 1*b*). The reversed solutions, $-K(X)$, are “antikinks.” These kinks and antikinks persist for much longer periods of time than the “evaporation fronts” which disappear after the rapid disintegration of the unstable phase. In Benney’s equation (2.1), they describe phase defects in the wave patterns (see Figure 1*b*) and are the central objects of the theory of defect dynamics (e.g. Coulet & Elphick 1989).

The real Ginzburg-Landau equation emerged from theories of superconductivity and phase transitions. On multiplying by $\partial_T a$ and integrating over X , we observe

$$-\int (\partial_T a)^2 dX = \frac{d}{dT} \int [(\partial_X a)^2 + \frac{1}{4}a^2(a^2 - 2x_2)] dX \equiv \frac{d}{dT} \mathcal{F} \tag{2.10}$$

Since the quantity \mathcal{F} is also bounded from below, it can be identified as

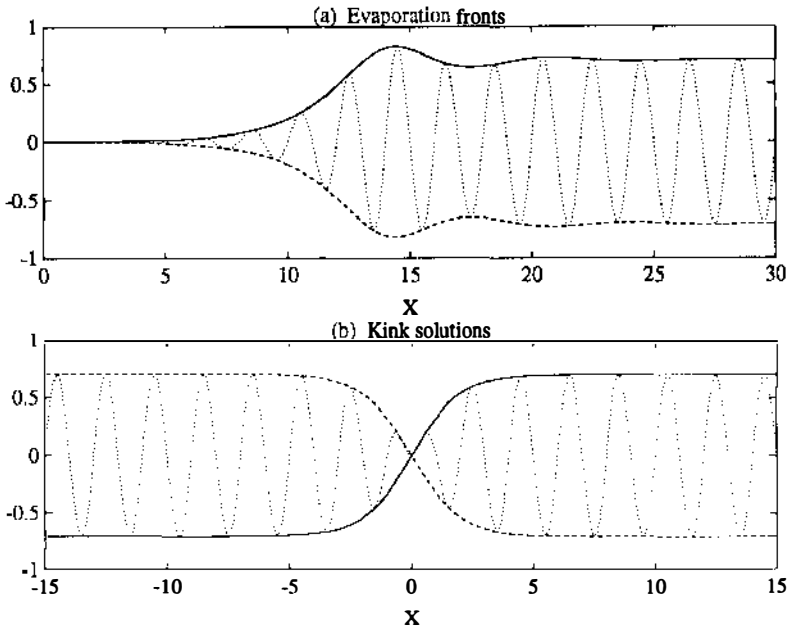


Figure 1 Illustration of kinks in the real Ginzburg-Landau equation. (a) An “evaporation front” connecting the unstable and stable phases. (b) A kink connecting the two stable phases. The continuous and dashed curves show $\pm A(X)$, and the dotted curve shows the corresponding waveform.

a Lyapunov Functional for the problem, and is commonly interpreted physically as a free energy.

Depending upon boundary conditions, the existence of \mathcal{F} implies that the asymptotic state of the system is typically one of the homogeneous, stable phases. This suggests that the equation is not interesting from the point of view of spatio-temporal complexity, which is not actually true. What often happens is that the evolution proceeds rapidly from some initial state as the unstable phase evaporates. This evaporation drives the system locally towards one of the two stable phases and leaves a metastable state consisting of multiple, phase-separated layers partitioned by a sequence of alternating kinks and antikinks. The metastable state eventually relaxes to the asymptotic state, but in the interim, a complicated, slowly evolving pattern emerges through a form of kink or frontal dynamics. Moreover, slight perturbations can sustain kink-antikink patterns indefinitely. We return to this topic in Section 4.

2.3 *The Cubic Schrödinger Equation*

In the limit of large dispersion, the large-amplitude solutions of (2.7) satisfy the cubic Schrödinger equation:

$$i\partial_{\tau}A = \partial_x^2 A + 2|A|^2 A \quad (2.11)$$

(again after rescaling). This equation has the soliton solution

$$A = ike^{-i(\Phi - \Phi_0)} \operatorname{sech} k(X - VT + X_0), \quad (2.12)$$

where the phase is given by

$$\Phi = \frac{1}{2}VX + \left(\frac{1}{4}V^2 - k^2\right)T, \quad (2.13)$$

which indicates that (2.12) is actually a two-parameter family of solitons with scale k and speed V , centered at X_0 with characteristic phase Φ_0 (e.g. Kivshar & Malomed 1989). One such soliton, which describes a localized packet or pulse of traveling waves, is shown in Figure 2.

The cubic Schrödinger equation is an integrable system, and its soliton solutions can be studied using inverse scattering techniques (Ablowitz & Segur 1981). This allows us to generate multiple solitary-wave equilibria and consider soliton dynamics within the framework of an exact theory. In the following sections we detail an approximate method dealing with just these issues for general, dissipative PDEs. More along these lines, one can use inverse scattering theory to deal perturbatively with weakly nonintegrable generalizations of (2.11). In particular, the physics of instability and dissipation appear as small forcing terms in (2.11) in the limit of large, but not infinite μ . Under such perturbations, inverse scattering

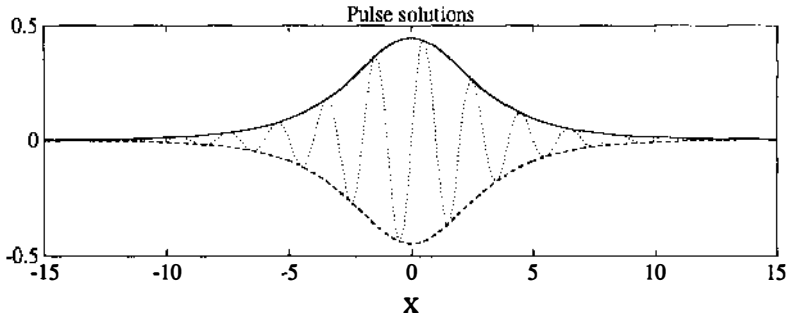


Figure 2 Illustration of a soliton in the nonlinear Schrödinger equation. The continuous and dashed curves show $\pm A(X)$, and the dotted curve shows the corresponding waveform.

theory leads to ODEs governing the evolution of the soliton's intrinsic parameters, i.e. its position X_0 , phase Φ_0 , scale k , and speed V (e.g. Kivshar & Malomed 1989).

2.4 Spatio-Temporal Chaos in Complex Ginzburg-Landau

For less specific choices of the coefficients, the complex Ginzburg-Landau equation displays a wide variety of behaviors involving coherent structures. In particular, it has become fairly important as an equation modeling spatio-temporal chaos. The phenomenon is characterized by at least two regimes (Shraiman et al 1992, Chaté 1994). Near the real Ginzburg-Landau limit, "phase turbulence" develops. This appears to be a state of weak disorder reflected in the phase of A . It is closely connected to spatio-temporal chaos in the Kuramoto-Sivashinsky equation (Kuramoto 1984), which was derived as a phase-evolution equation for complex Ginzburg-Landau under certain conditions. The Kuramoto-Sivashinsky equation is the dispersionless special case of equation (2.1) and we consider it again in Section 4. In fact, in a more appropriate, moving reference frame, the phase evolution equation for complex Ginzburg-Landau turns out to be precisely Equation (2.1) but with an additional higher-order nonlinear term (Janiaud et al 1992). Phase turbulence seems to be associated with propagating shocks or fronts in A , and pulses in the gradient of the phase of A .

Near the highly dispersive limit, the characteristics of spatio-temporal chaos have been labeled "dispersive chaos" (Kolodner et al 1990) or "defect turbulence" (Shraiman et al 1992). The main features associated with such a state appear to be pulses that are briefly coherent in space and time. They arise through intense "self-focusing" by dispersion and subsequent breaking by dissipation (Bretherton & Spiegel 1983). In the nonlinear Schrödinger limit, these pulses probably become the solitons

(2.12). Under suitable forcing, the weakly nonintegrable dynamics of these solitons does show chaotic characteristics resembling the dispersive chaos of the complex Ginzburg-Landau equation (Nozaki & Bekki 1986).

Pulses, fronts, and related complex solutions are also commonly encountered in studying generalizations of the complex Ginzburg-Landau appropriate to subcritical Hopf bifurcations. A more complete survey of pulses and fronts in this kind of equation is given by van Saarloo & Hohenberg (1993).

3. PULSE-TRAIN EQUILIBRIA

3.1 *Pulse Trains and Spacing Maps*

The arguments of the previous section concerning the common kinds of solutions to the complex Ginzburg-Landau equation suggest that Hopf bifurcations (whether subcritical or supercritical) often lead to the formation of propagating, coherent structures in spatially extended systems. Furthermore, complexity of a variety of kinds is associated with them.

For Equation (2.1) with $\alpha = 0$, the spatially extended state bifurcates to instability with zero frequency. A Hopf bifurcation occurs, however, for spatially periodic systems as the domain size increases through a critical value (Elphick et al 1991a). The unstable modes saturate supercritically as nonlinear waves. They develop into pulses on increasing the domain size further, thus illustrating how spatially periodic systems also form coherent structures. We now direct our attention to such situations.

We journey into a theory of the patterns created by an ensemble of solitary waves, focusing upon pulses rather than kinks (minor modifications are required to treat the latter). We outline a singular perturbation theory to derive multiple solitary-wave trains, or bound states of pulses [an alternative procedure is the variational technique discussed by Kath et al 1987 (see also Ward 1992)]. We leave the question of boundary conditions and stability until Sections 4 and 5.

When we introduce a traveling-wave coordinate $\xi = x - ct$ into (2.1) and integrate once, we find the ODE

$$\left(\frac{d^3}{d\xi^3} + \mu \frac{d^2}{d\xi^2} + \frac{d}{d\xi} \right) \Xi - c\Xi + \frac{1}{2}\Xi^2 = 0 \quad (3.1)$$

for the steady pulse train solutions, where $\Xi(\xi) = u(x, t)$.

The singular perturbation expansion centers around the idea that trains consist of widely separated pulses. The component pulses are weakly distorted versions of the true solitary waves. Single-pulse solutions centered at various positions within the train can therefore be used as a

leading-order approximation to the pattern's structure (cf McLaughlin & Scott 1978, Gorshkov & Ostrovsky 1981, Kawasaki & Ohta 1982, Gold'shtik & Shtern 1981, Coulet & Elphick 1989).

We let the single-pulse solution be denoted by $H(\xi)$, and choose the origin so that $H(\xi)$ has its principal peak at $\xi = 0$. Away from the main peak, the pulse amplitude falls approximately exponentially. At the position of the preceding and following pulses, we assume that the amplitude is of order ε . This means that the overlap of neighboring pulses is $O(\varepsilon)$, and so the intrinsic structure of each pulse is $H(\xi) + O(\varepsilon)$. We illustrate this in Figure 3, and write the ansatz

$$\Xi(\xi) = \sum_k H(\xi - \xi_k) + \varepsilon R + O(\varepsilon^2), \tag{3.2}$$

where ξ_k denotes the positions of the pulses and εR is an error correction term. Were they in isolation, the pulses would move at a speed c_0 . However, through interaction between the component pulses, the pattern translates differently, and $c \neq c_0$, but the disparity is small and $c = c_0 + \varepsilon c_1 + O(\varepsilon^2)$, where c_1 is order unity.

We now introduce the expansion (3.2) into the basic Equation (3.1) and divide that equation into relations of distinct orders in ε . The leading-

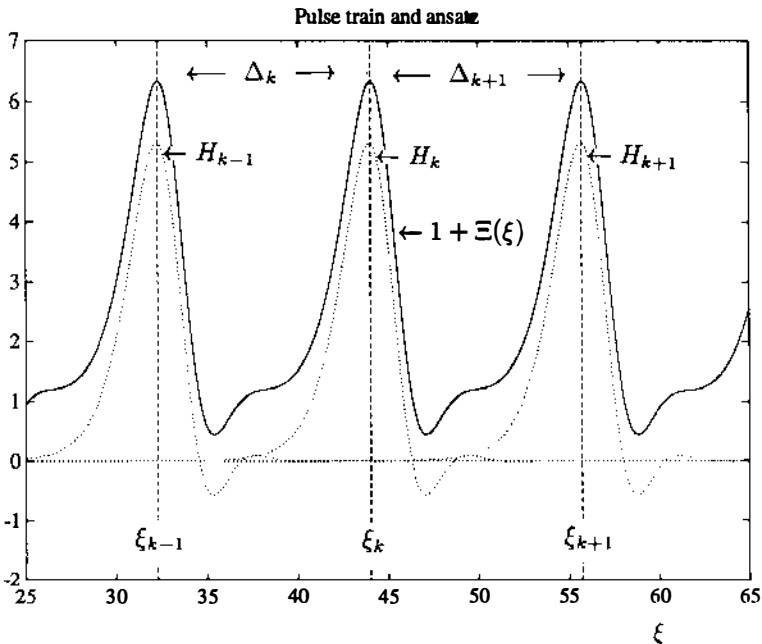


Figure 3 An illustration of the pulse train and ansatz [$H_k = H(\xi - \xi_k)$].

order equation is just that for the various single-pulse solutions. The equation at next order is a linear inhomogeneous equation for R . It has secularly divergent particular solutions unless we enforce a solvability condition upon the positions of the pulses. This condition is

$$c_1 = F(\xi_k - \xi_{k-1}) + F(\xi_k - \xi_{k+1}), \quad (3.3)$$

where

$$F(\Delta) = \frac{1}{\epsilon I} \int_{-\infty}^{\infty} N(\xi') H(\xi') H(\xi' + \Delta) d\xi', \quad (3.4)$$

$N(\xi)$ is an adjoint null vector related to $H(\xi)$, and

$$I = \int_{-\infty}^{\infty} N(\xi') H(\xi') d\xi' \quad (3.5)$$

(e.g. Elphick, Meron & Spiegel 1990). In deriving this equation, we have tacitly assumed that the rate of decay of the pulse amplitude both fore and aft is approximately the same.

The quantities $\Delta_k \equiv \xi_k - \xi_{k-1}$ and $\Delta_{k+1} \equiv \xi_{k+1} - \xi_k$ are just an adjacent pair of pulse spacings, and so

$$F(\Delta_k) + F(-\Delta_{k+1}) = c_1 \quad (3.6)$$

determines the separations of the pulses as a map of the interval of Δ to itself. This is the spacing map from which we can build a pulse train. Before considering this map any further we briefly digress into the geometrical aspects of the pulse-train solution in the phase space of the dynamical system described by (3.1).

3.2 Pulse Trains as Dynamical Systems

In order to apply the theory described above, we need to know the various kinds of single-pulse solutions, $H(\xi)$, that can arise. To find these we must study the ODE (3.1) in a little more detail.

In the phase space, $\mathbf{U} = (\Xi, \Xi', \Xi'')$, Equation (3.1) describes a velocity field, $\mathbf{V} = \mathbf{U}'$ (where $'$ indicates differentiation with respect to argument). The divergence of the velocity field is just $-\mu$ indicating that, for $\mu > 0$, the flow is volume contracting; as ξ advances, an arbitrary set of initial points in phase space gradually condenses into a region of zero volume. Provided solutions remain bounded, the geometry restricts that region to be either a point, a curve, or some complicated object of dimension less than three. In other words, the system asymptotically heads towards an

attractor, which could be a fixed point, a periodic orbit, or a strange attractor.

The attractors of the system are dependent upon the parameters of Equation (3.1). In the context of this ODE, the parameters are μ and c (for the PDE, c is the pattern speed and only μ is a parameter). These form a two-dimensional parameter space in which the various attractors reside. They are destroyed or created at certain conjunctions or bifurcations, and the possibilities admitted by (3.1) are complicated (Arneodo et al 1985b, Glendinning & Sparrow 1984).

A sample sequence of bifurcations is shown in Figure 4, which shows the succession of states that are realized as c is varied for $\mu = 0.7$. Initially

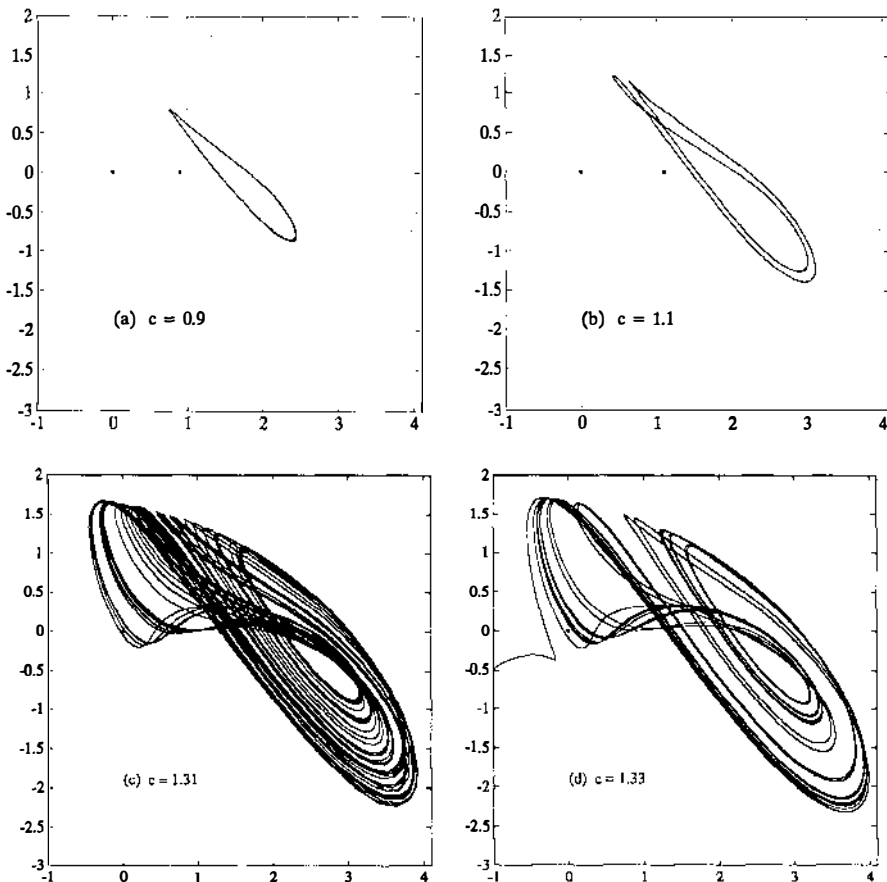


Figure 4 Bifurcation sequence of Equation (3.1) for $\mu = 0.7$ and four values of c . The four panels show phase portraits projected onto a plane with coordinates $(\xi, \zeta + \zeta/4)$. The stars mark the fixed points. (Based on Arneodo et al 1985b.)

the system contains two fixed points. That at the origin, $\Xi = 0$, is a saddle, and the nontrivial fixed point, $\Xi = 2c$, is a stable focus. Increasing c eventually destabilizes the focus, and it sheds a limit cycle (Figure 4a). This cycle then bifurcates to a second cycle with twice its frequency (Figure 4b) and there follows a period-doubling cascade leading to the complicated object shown in Figure 4c, which we interpret to be a strange attractor (though this is not rigorously shown). This object develops as we raise c again, eventually colliding with the origin. Shortly after this point (Figure 4d), the trajectories beginning from points in the half-space $\Xi > 0$ can find their way along a chaotic trajectory into $\Xi < 0$, and diverge to $\Xi = -\infty$ since the nonlinear term Ξ^2 cannot then saturate growth in amplitude.

In this fashion, the various attractors of the system and their bifurcations can be catalogued to visualize the kinds of propagating patterns that solve (3.1). Of primary interest in the current context are the solutions that describe localized structures like pulses and kinks. These solutions necessarily approach constant amplitude as $\xi \rightarrow \pm\infty$, and so they must asymptote to the fixed points. The solutions that connect a fixed point to itself are the *homoclinic* orbits of the system. In real space and time, these define propagating pulses. The *heteroclinic* orbits connect different fixed points and represent kinks. Some examples are shown in Figure 5.

The homoclinic trajectory shown in Figure 5 connects the origin to itself. It can therefore be created by a bifurcation in which a periodic orbit collides with the origin. The details of this bifurcation are uncovered using Shil'nikov theory as we elaborate soon, but the locations of some of these orbits in parameter space are already suggested from the sequence shown in Figure 4. The object shown in Figure 4c is filled with unstable periodic orbits. When it collides with the origin these periodic orbits begin connecting $\Xi = 0$ and consequently become homoclinic. For any one periodic orbit, the point of bifurcation in c typically defines a unique point at fixed μ in parameter space; this is simply the solitary-wave speed, c_0 . For varying μ , we expect a curve on the parameter plane, $c_0(\mu)$.

3.3 Homoclinic Dynamics

Except for a relatively short interval, the homoclinic solution shown in Figure 5, $H(\xi)$, is contained within the neighborhood of the origin. Here, Equation (3.1) can be approximately replaced by its linearization and we find the solution

$$\Xi \simeq ae^{\sigma\xi} + be^{-\gamma\xi} \cos(\omega\xi + \psi), \quad (3.7)$$

where σ and $-\gamma \pm i\omega$ are the eigenvalues of the flow, and a , b , and ψ are constants. The homoclinic connection emerges from the origin O at

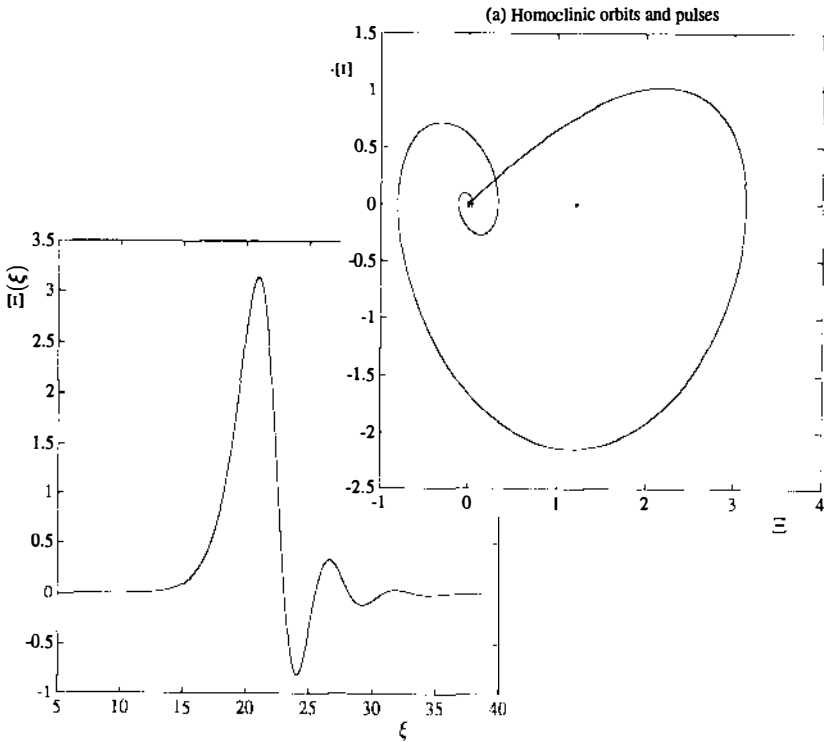


Figure 5 Illustrations of the homoclinic and heteroclinic solutions of (3.1). (a) A homoclinic orbit and its pulse-like "time trace." (b) A heteroclinic orbit and its frontal "time trace." The orbits are shown projected onto the (Ξ, ξ) plane. The stars shown the fixed points. (Based on Balmforth et al 1994, Conte & Musette 1989.)

$\xi = -\infty$, escapes the vicinity of the origin, but rapidly returns and spirals back into O at $\xi = \infty$. Thus

$$H(\xi) = \begin{cases} a_0 e^{\sigma \xi} & \xi \rightarrow -\infty \\ b_0 e^{-\gamma \xi} \cos(\omega \xi + \psi_0) & \xi \rightarrow \infty \end{cases} \quad (3.8)$$

The two sections of the solution for H correspond to two invariant manifolds intersecting O : a one-dimensional unstable manifold and a stable two-dimensional manifold. The homoclinic orbit is the intersection of these two manifolds.

Nearly homoclinic trajectories typically get caught near the invariant manifolds, and consequently they "skirt" $H(\xi)$ during any excursion away from O . But since they generally do not reenter the vicinity of the origin

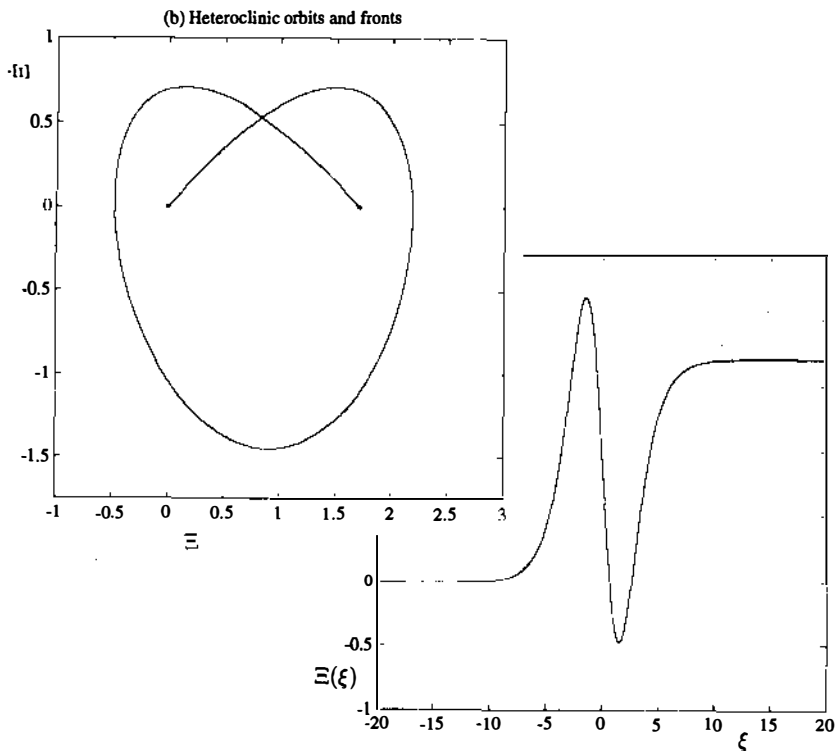


Figure 5b.

with $a = 0$ identically, the trajectories do not fall into $\Xi = 0$. Instead they become thrown out from the origin's vicinity along the unstable manifold after spending a lengthy period there. Because the reinjection process is relatively rapid, the solution $\Xi(\xi)$ takes on the appearance of a train of widely separated pulses, as illustrated in Figure 6. Two trajectories begin on the unstable manifold. One defines the homoclinic connection. In the second, that connection is broken with $c = c_0 + \varepsilon c_1$, and the trajectory proceeds into further pulses after the first.

The nearly-homoclinic solutions spend long durations circulating near the origin, where we have solution (3.7). The main peak of the pulse, on the other hand, shadows the homoclinic's loop and $\Xi(\xi) \simeq H(\xi)$. This means that the solution is relatively insensitive to the details of the path taken away from the origin, but is critically controlled by the flow near $\Xi = 0$. By connecting the solutions in these two representative regions, we furnish an approximation for the pulse train. This geometrically motivated

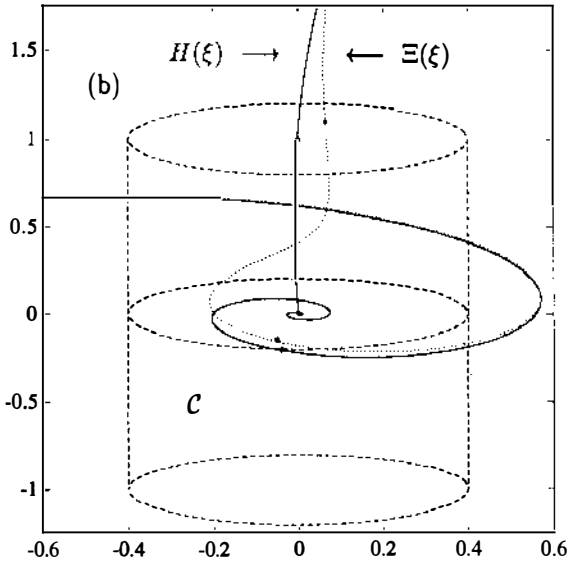
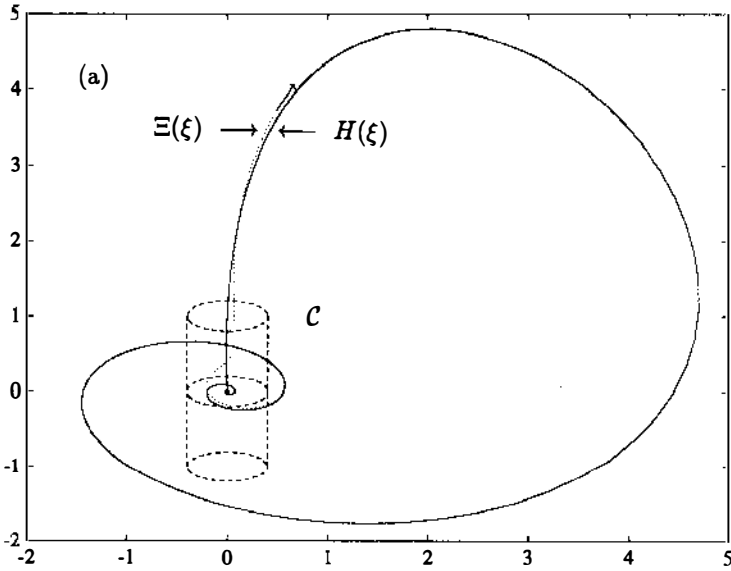


Figure 6 An illustration of homoclinic dynamics. (a) A homoclinic orbit $H(\xi)$ and a nearly homoclinic trajectory $\Xi(\xi)$ beginning from the unstable manifold of the origin. The cylindrical central region \mathcal{C} is identified. (b) Magnification of the region surrounding \mathcal{C} .

analysis, or Shil'nikov theory (Shil'nikov 1965, 1970; Tresser 1984a), provides a parallel description to singular perturbation theory.

3.4 *Shil'nikov Theory*

The flow portrayed in Figure 6 surrounds the unstable manifold emerging from the origin. In the homoclinic condition, this manifold connects to the stable manifold. In the nearly homoclinic conditions in which we operate, the two manifolds do not meet, but twist around one another in a complicated geometrical way. We visualize the dynamics of the flow by placing a surface through the phase space and determining the succession of intersections of a trajectory with it. This surface is an example of a Poincaré section. Moreover, the relation between the coordinates of successive intersections is a return map which completely characterizes the flow.

Within the cylindrical region \mathcal{C} , the flow is approximately given by the linear system:

$$\dot{x}_1 = -\sigma x_1 + \omega x_2, \quad (3.9)$$

$$\dot{x}_2 = -\sigma x_2 - \omega x_1, \quad (3.10)$$

and

$$\dot{x}_3 = \gamma x_3, \quad (3.11)$$

with σ , ω , and γ real and positive. There is a linear transformation between the two sets of coordinates, \mathbf{U} and (x_1, x_2, x_3) . In this way, the coordinate axes of \mathbf{x} are the invariant manifolds of the flow within \mathcal{C} . In particular, the homoclinic orbit departs \mathcal{C} along the x_3 axis, then returns and spirals back into O in the x_1 - x_2 plane. Likewise, the flow leaves \mathcal{C} through its top surface, shadows the homoclinic orbit, and then reenters the vicinity of the origin through the lateral surface of \mathcal{C} .

The central domain \mathcal{C} is bounded by the surfaces $x_1^2 + x_2^2 = \varepsilon^2 r^2$ and $x_3 = \varepsilon Z_0$. Within it, the flow geometry is given by

$$x_1 = \varepsilon r e^{-\sigma(\xi - \tilde{\xi}_k)} \sin[\omega(\xi - \tilde{\xi}_k) + \varphi_k], \quad (3.12a)$$

$$x_2 = \varepsilon r e^{-\sigma(\xi - \tilde{\xi}_k)} \cos[\omega(\xi - \tilde{\xi}_k) + \varphi_k] \quad (3.12b)$$

and

$$x_3 = \varepsilon Z_k e^{\gamma(\xi - \tilde{\xi}_k)}, \quad (3.12c)$$

for some φ_k , $\tilde{\xi}_k$, and Z_k . $\tilde{\xi}_k$ records the "time" of reinjection into \mathcal{C} , the instant when the trajectory intersects the curved surface. This surface acts

as our Poincaré section, and Z_k and φ_k are the section's (curvilinear) coordinates.

Trajectories exit \mathcal{C} at the top surface and the interval in ζ spent within \mathcal{C} is given by

$$T_k = -\frac{1}{\gamma} \log(Z_k/Z_0). \tag{3.13}$$

It now remains to connect the values of φ_k and Z_k with their subsequent values. In Shil'nikov theory, one normally makes some simplifying assumptions regarding the flow outside \mathcal{C} . This amounts to linearly relating the coordinates on the upper surface of \mathcal{C} to φ_{k+1} and Z_{k+1} (e.g. Arneodo et al 1985b), and leads to

$$\varphi_{k+1} = \varphi_0 + qe^{-\sigma T_k} \sin(\omega T_k + \varphi_k + \Psi_1) \tag{3.14}$$

and

$$Z_{k+1} = \varepsilon C + Qe^{-\sigma T_k} \sin(\omega T_k + \varphi_k + \Psi_2), \tag{3.15}$$

where φ , C , q , Q , Ψ_1 , and Ψ_2 are constants. These two equations constitute a map of the Poincaré section into itself: the advertised return map. Because of the simplifications, the constants are not defined in closed form and are normally treated as parameters.

3.5 Return Maps vs Spacing Maps

Although we suggested earlier that the two ways to analyze pulse train equilibria ran parallel, the spacing map (3.6) is quite clearly not equivalent to the two-dimensional return map (3.14)–(3.15). The reason for this is that the Shil'nikov theory is not strictly consistent in retaining terms of similar asymptotic order. In order for the pulses to be widely separated, the interval in ζ spent within \mathcal{C} must be longer than the traversal interval outside it. This means that T_k is relatively long, and so the exponentials $\exp(-\sigma T_k)$ are small—in fact of order ε . Glancing back at Equation (3.14) for the phase coordinate φ_{k+1} reveals that, to this order, $\varphi_k \sim \varphi_0$, and so

$$Z_{k+1} = \varepsilon C + Qe^{-\sigma T_k} \sin(\omega T_k + \varphi), \tag{3.16}$$

where $\varphi = \varphi_0 + \Psi_2$ and T_k is given by (3.13). This is a map of the interval, and arises from what amounts to a local, strong “contraction” of nearby points in phase space towards the curve $\varphi_k = \varphi_0$ on the Poincaré section.

The interval spent outside \mathcal{C} is essentially a constant, ξ_R , and so the “flight time” between the successive intersections with the Poincaré section is $\Delta_k = T_k + \xi_R$. When we use this quantity as the iterative variable, the

map takes the form of a spacing map. It is identical to (3.6) if the functions $F(\Delta)$ are evaluated using the asymptotic solution given by (3.8) and $c_1 = \varepsilon C$.

In the limit of widely separated pulses, the two approaches therefore lead to similar results. Singular perturbation theory is more powerful than conventional Shil'nikov theory in that one can compute the function $F(\Delta)$ without any free parameters (though in principal we could extend Shil'nikov's theory). Shil'nikov analysis reveals that the underlying map describing the flow is truly two-dimensional, and it is only through strong contraction that it appears one-dimensional. As a consequence, the spacing maps that one extracts from numerical solution of an ODE like (3.1) appear one-dimensional only to leading order in ε , and have hidden fractal structure (Balmforth et al 1994).

3.6 Bifurcation Theory

The one-dimensional return map (3.16) is often called Shil'nikov's map. We write it more explicitly as

$$Z_{k-1} = C + BZ_k^\delta \sin(\Omega \log Z_k + \Phi) \equiv f(Z_k), \quad (3.17)$$

where B and Φ are constants, $\delta = \gamma/\sigma$, and $\Omega = \omega/\delta$. The map is illustrated in Figure 7 for $C = 0$ in the two cases $\delta > 1$ and $\delta < 1$.

Periodic orbits intersect the Poincaré section at a distinct set of points and appear as recurrent iterations in the map. The fixed points of the map, $Z = Z_k = Z_{k+1} = f(Z)$, correspond to the lowest-order periodic orbits of (3.1). Such orbits hit the Poincaré section at a single point, and their periods follow from $\Pi = \xi_R - \log(Z/Z_0)/\gamma$. If we view C as a bifurcation parameter, then (3.17) predicts the behavior of the periodic orbit as C scans through the homoclinic value, and reveals the bifurcation sequence that creates $H(\xi)$ (Glendinning & Sparrow 1984).

When $\delta > 1$, there is a single orbit for which Z monotonically approaches 0 as C decreases to homoclinicity. The orbital period Π simultaneously diverges (inset of Figure 7a). In other words, the homoclinic connection is created by a single periodic orbit colliding with the origin.

For $\delta < 1$, a periodic orbit winds into homoclinicity through an infinite sequence of saddle-node bifurcations (inset of Figure 7b). Moreover, shortly beyond each saddle-node bifurcation along the locus, there are period-doubling cascades (Glendinning & Sparrow 1984). This sequence of bifurcations generates infinitely many unstable periodic orbits at $C = 0$. In the vicinity of the homoclinic connection, we therefore predict the existence of a chaotic, dense set (i.e. the union of the unstable periodic orbits). This is the essence of Shil'nikov's theorem for $\delta < 1$ (Shil'nikov

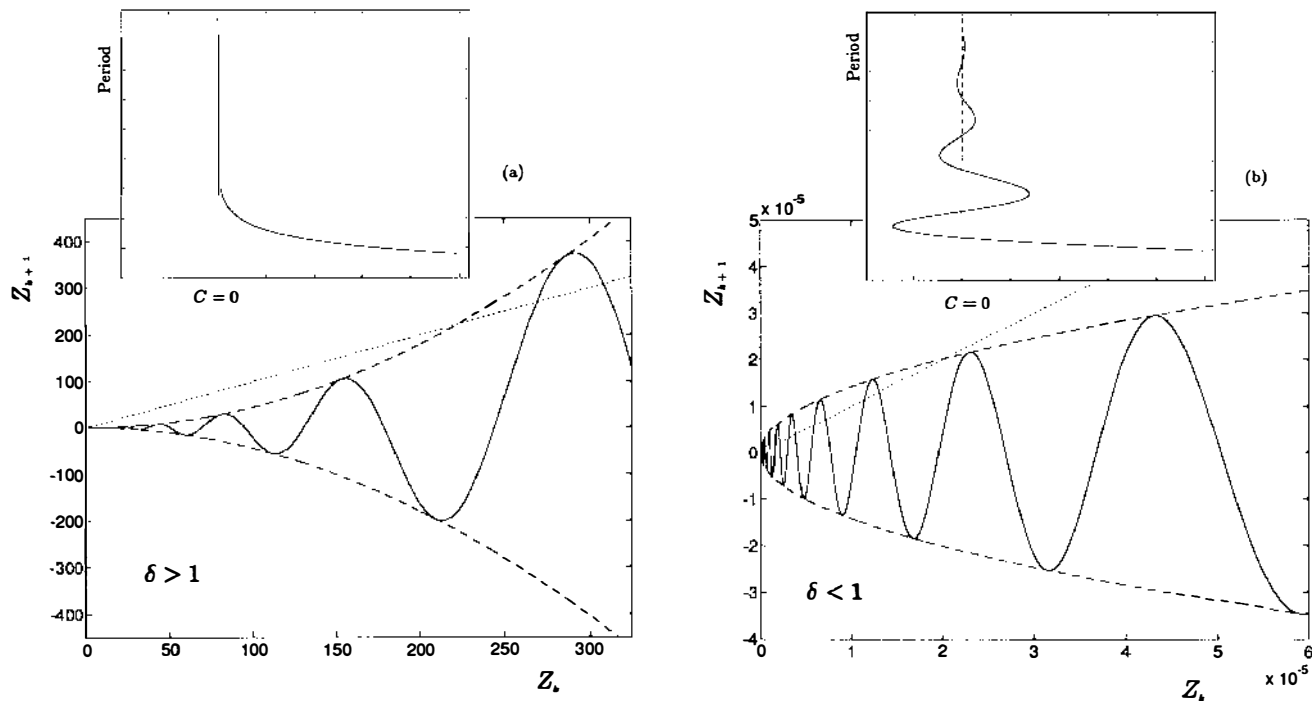


Figure 7 An illustration of Shil'nikov's map for (a) $\delta = 2$ and (b) $\delta = 0.5$. The inset panels picture the behavior of a fixed point of the map as C varies. (Based on Glendinning & Sparrow 1984.)

1965, 1970; Tresser 1984a). In this region of parameter space we anticipate chaos, although the long-term stability of the set is not determined by the theorem and we cannot claim the existence of a strange attractor. If such an object nevertheless exists, we find “Shil’nikov” or “homoclinic chaos,” which is observed as a train of irregularly spaced pulses: steadily propagating, spatially chaotic patterns in the PDE.

3.7 Sample Spacing Maps and Homoclinic Chaos in Other Systems

In the context of our current example, the ODE (3.1), it is actually fairly difficult to find strange attractors near the homoclinic bifurcation. Figure 8 shows a sample pulse train and its spacing map. The asymptotic map agrees with numerically determined spacings, and both terminate after a short sequence of pulses. The train terminates because the trajectory of the solution finds a way around the stable manifold at the origin and then diverges to $\Xi \rightarrow -\infty$. On the map, the final iteration reaches negative values for Z , implying that the trajectory exits the domain \mathcal{C} of Figure 6 through its lower surface and fails to return. Such divergence leads to the gaps that are evident in the spacing map of Figure 8b.

Although the generic behavior of the pulse train is to terminate, by judiciously using the map, one can nevertheless find trains that continue indefinitely. This amounts to locating intervals in Z or Δ that remain invariant under the action of the map, but they constitute a tiny part of the phase space and their basins of attraction are small.

Although we have approached the problem from the physical point of view of spatial complexity in solitary wave patterns, homoclinic chaos is relevant also to systems that can be described simply by ODEs. For example, in modal approximations of fluid convection, Arneodo et al (1985a) and Knobloch & Weiss (1983) observed homoclinic behavior. Further examples, and even experimental indications, of homoclinic chaos are described in a recent conference proceedings (*Physica* 62D).

The divergent behavior associated with trajectories rounding the stable manifold at the origin can be avoided if Equation (3.1) contains a different nonlinear term. In particular, if we replace Ξ^2 with a cubic nonlinearity, the equation gains the symmetry $\Xi \rightarrow -\Xi$ and becomes identical to the model considered by Arneodo et al (1985a). Then the homoclinic orbit $H(\xi)$ has a mirror image, $-H(\xi)$. Traversal of the stable manifold now leads to an “anti-pulse” rather than divergence, and the prospect of finding global strange attractors is more promising. A solution of the equation with cubic nonlinearity is shown in Figure 9. In this case, the unmodified spacing or timing map contains no gaps, but it is double-valued (the Z -map is not—Glendinning 1984, Balmforth et al 1994). This cubic ODE

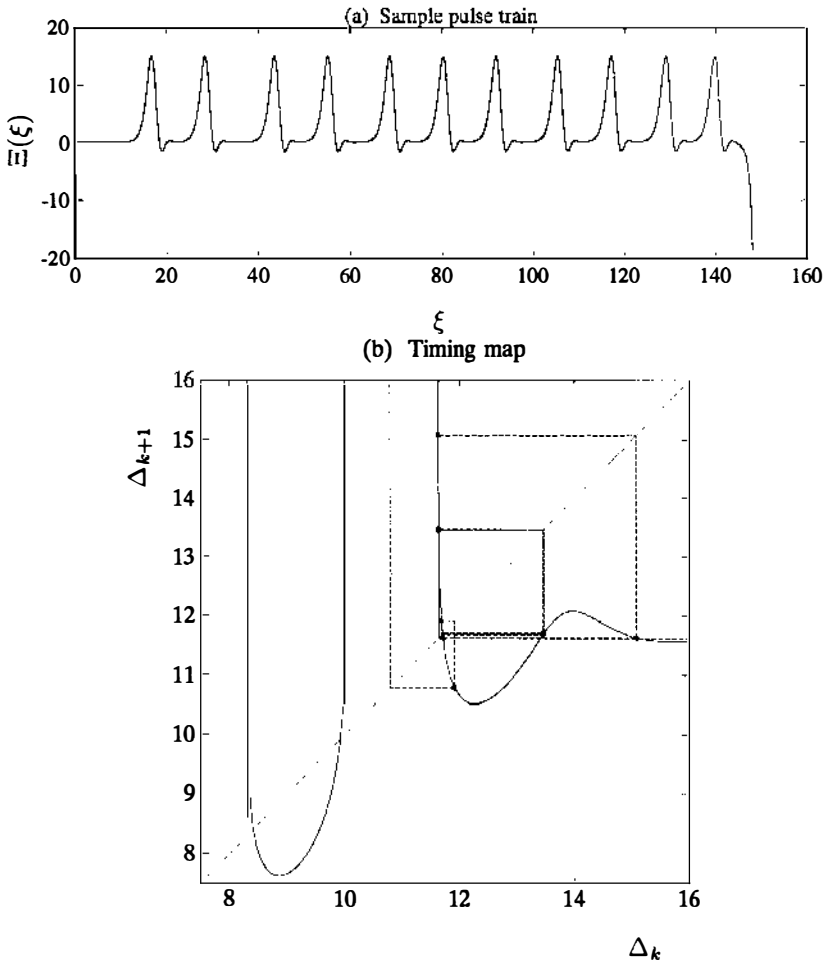


Figure 8 (a) Sample pulse train and (b) the associated spacing map. The curves indicate the asymptotic map; the stars and iteration show the computed spacings. $\mu = 1/\sqrt{2}$ and $c = 1.92847$. (Based on Balmforth et al 1994.)

also describes the steady traveling wave solutions of a *modified* version of (2.1), a model which arises in other fluid dynamical contexts (Tilley et al 1992).

The existence of the anti-pulse in the symmetrical version of (3.1) amounts to the presence of a mechanism that reinjects trajectories back into the vicinity of the origin on either side of the stable manifold. The reinjection process need not be nearly homoclinic, nor does it guarantee the asymptotic stability of the homoclinic strange set. In fact, the object

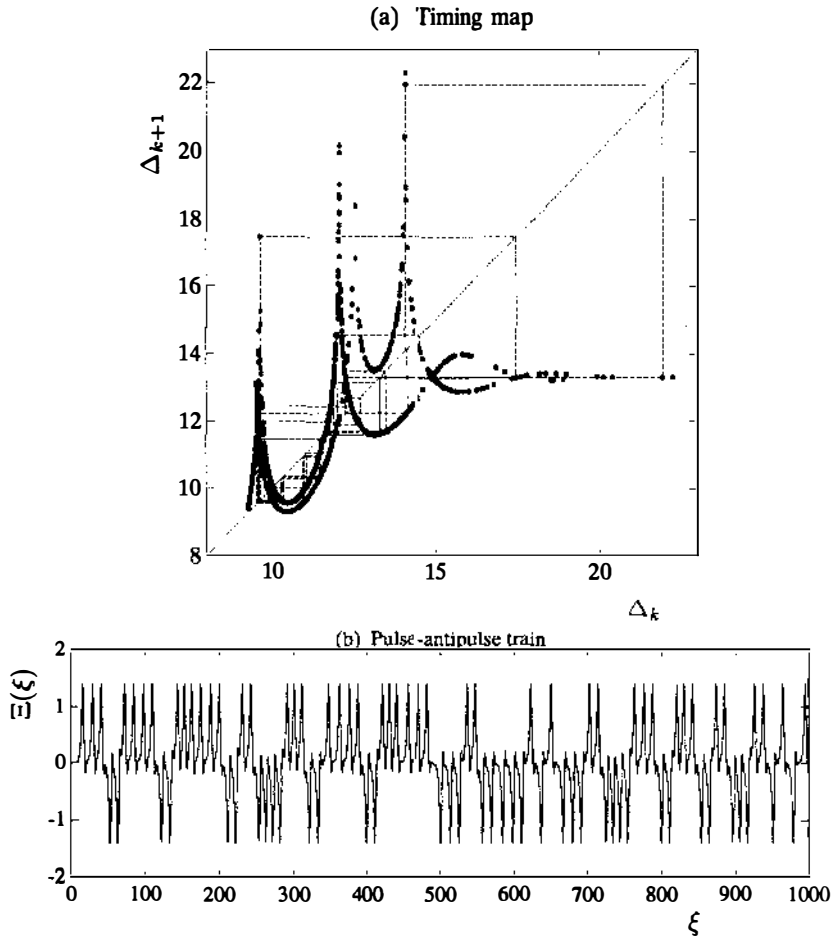


Figure 9 An invariant set for Equation (3.1), but with cubic nonlinearity. $\mu = 0.7$ and $c = 1.1$. (a) Empirical (measured) spacing or timing map. A sample iteration is also plotted as the dashed lines, and the diagonal is drawn as the dotted line. (b) Part of the pulse-antipulse train. (c) Phase portrait projected onto the $(\Xi, \dot{\Xi})$ plane. The stars indicate the fixed points. (Based on Balmforth et al 1994.)

shown in Figure 9 does not even satisfy Shil'nikov's criterion for the existence of a strange set (parameters are chosen such that $\delta > 1$), yet it is probably a strange attractor.

3.8 Variations

In the example we have considered so far, we have the image of Figure 6; the homoclinic orbit ascends from the origin along the one-dimensional

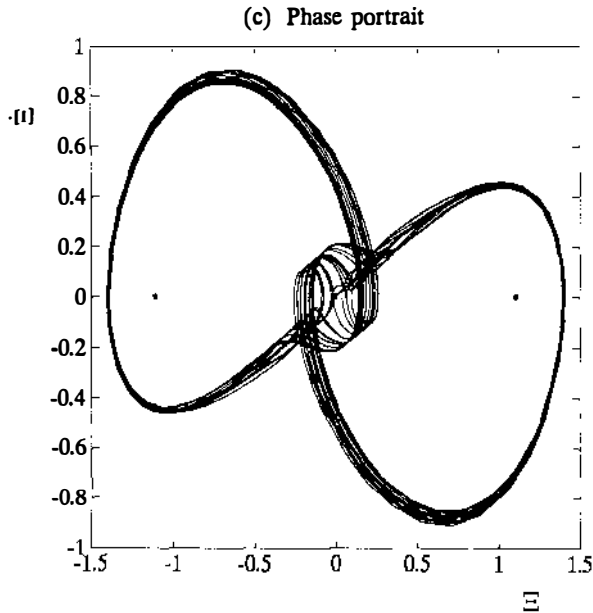


Figure 9c.

unstable manifold, and then returns in a decaying spiral within the two-dimensional stable manifold. A somewhat different picture emerges when the homoclinic trajectory winds out of the origin and descends monotonically back in. The pulse is a reversed version of our original image, and we refer to it as an “inverse Shil’nikov” orbit. A chaotic solution beginning near such an object is shown in Figure 10 [generated from a piecewise linear equation of Tresser (1981)]. The trajectory occasionally approaches the homoclinic orbit in this example, but more often than not,

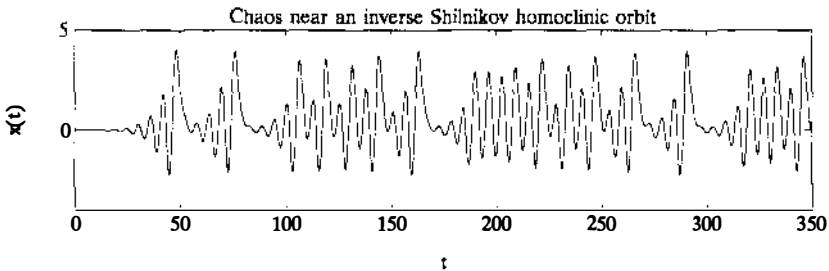


Figure 10 The time trace of a chaotic solution in the vicinity of an inverse Shil’nikov homoclinic orbit (adapted from Tresser 1981). Not shown is a nearly homoclinic precursor.

it wanders well away from it. As a result, the solution does not resemble a train of widely separated pulses and is difficult to analyze with singular perturbation theory. Argoul et al (1987) attempted Shil'nikov theory for these reversed orbits and interpreted experimental data from a chemical reaction in terms of "inverse" Shil'nikov chaos.

Pulses also need not possess oscillatory tails to either the fore or aft if the system is to admit potentially chaotic solutions. In particular, monotonically decaying homoclinic orbits are frequently encountered in systems like the Lorenz equations (e.g. Sparrow 1982). There, the counterpart of Shil'nikov theory has been widely adapted to understand some of the bifurcations leading to the Lorenz and related attractors (although typically those attractors themselves are far from being in a homoclinic condition). Tresser (1984b) summarizes the various kinds of homoclinic situations for flows in three dimensions.

Shil'nikov theory can also be adapted to study higher-dimensional systems. In four dimensions one anticipates homoclinic orbits connecting the two-dimensional stable and unstable manifolds of the origin (Glendinning & Tresser 1985). Fowler & Sparrow (1991) have derived return maps expected in the case when the pulses wind both in and out of the origin. Typically, these are maps of the plane and not simple, one-dimensional Shil'nikov maps. If we follow singular perturbation theory, it is not immediately clear how we can account for this, since the analysis proceeds without any explicit statement regarding dimension, and so the theory predicts the one-dimensional spacing map (3.6) even for bifocal homoclinic orbits. There is currently little work on these higher dimensional pulses; Champneys & Toland (1993) have recently found bifocal homoclinic orbits in certain Hamiltonian systems.

A different step up in complexity is provided by bifurcation off the homoclinic orbit itself. Under suitable conditions, the homoclinically connected origin can lose stability altogether. If this occurs through a Hopf bifurcation, then the origin sheds a limit cycle. The stable and unstable manifolds of this limit cycle can play similar roles to the original manifolds of the origin, and in the same fashion that the original homoclinic orbit was established, they can intersect one another. This creates a "Shil'nikov-Hopf" homoclinic orbit which connects the limit cycle to itself (e.g. Gaspard & Wang 1987), and we can again use Shil'nikov theory to study the dynamics nearby (Hirschberg & Knobloch 1993).

These examples serve to illustrate the variety of homoclinic behavior, and each type of orbit can arise as a solitary wave solution of a PDE. This suggests that patterns of propagating pulses can comprise many different kinds of spatial complexity.

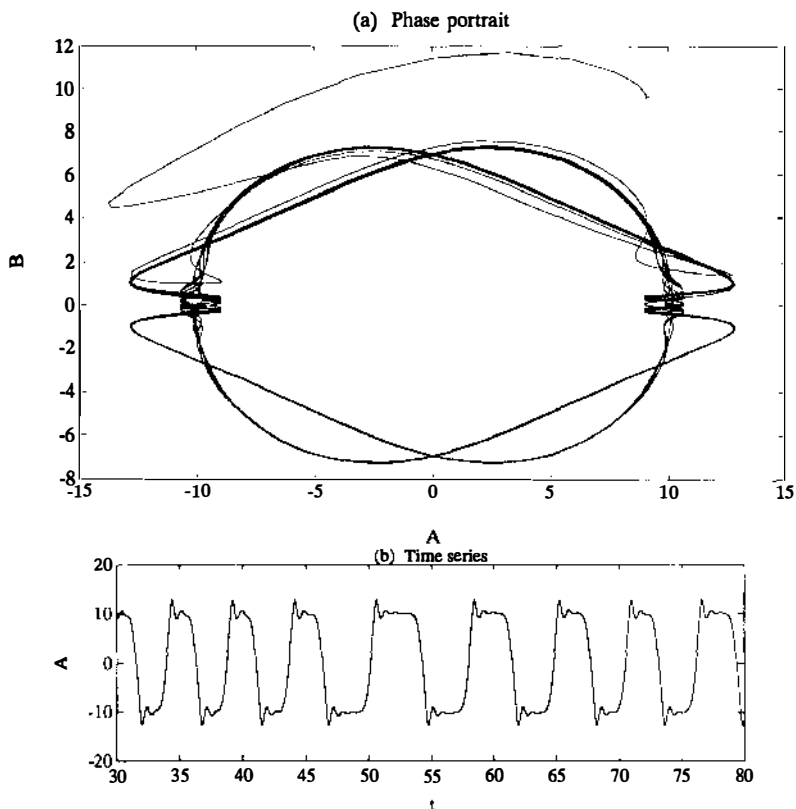


Figure 11 Heteroclinic chaos in the Howard-Krishnamurti model. (a) Phase portrait projected onto the (A, B) plane, where A and B are two of the variables of Howard & Krishnamurti (1986). (b) Time trace of A . (c) Empirical (measured) timing map. The first few iterations are indicated by the dashed lines, and the dotted line is the diagonal. (Based on Howard & Krishnamurti 1986; their parameter values are $\sigma = 1$, $\alpha = 1.2$, and $R = 86$.)

The richness associated with homoclinic dynamics also carries over to situations with heteroclinic connections. For these we can again develop Shil'nikov theory, and under suitable conditions we then predict "heteroclinic chaos," again with reservations concerning asymptotic stability. Along these lines, Howard & Krishnamurti (1986) found strange attractors related to heteroclinic connections in ODEs that model shearing convection. Figure 11 shows a solution computed from that system and its spacing or timing map. For spatio-temporal systems, heteroclinic chaos corresponds to steadily propagating patterns of irregularly spaced fronts or kinks (cf Kopell & Howard 1981).

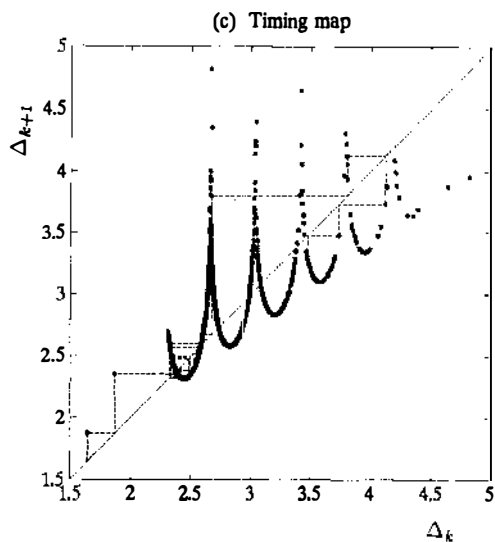


Figure 11c.

4. PULSE DYNAMICS

4.1 *Pulse Interactions*

In the previous section we began by discussing steadily propagating pulse trains. We then digressed substantially into the theory of homoclinic orbits. Now we return to the more physical aspects of pulses, and consider the dynamical evolution of patterns of pulses by extending the methods of the last section.

In order to make the problem tractable from an analytical point of view, we restrict ourselves to consider only certain kinds of pulse dynamics. In what follows, we envision an ensemble of pulses which are nearly locked into a steadily propagating pattern. However, through an initial perturbation, or perhaps an intrinsic instability, the pulses within the pattern are in a state of dynamical adjustment. This probably precludes the kinds of dynamics familiar in integrable systems, like soliton collisions. Just as importantly, we also cannot cope with pulse creation and destruction (the former of which is critical to the pulses of Benney's equation, as we shortly indicate). But to take these effects into account, we need another theory, and one is not yet available. An alternative way around this is to "patch" numerical solutions into the asymptotic theory when necessary. In this way Ward (1994) treated front collisions by substituting a numerical solution whenever the fronts approached another too closely.

The assumption of weak adjustment means that the pulses of the pattern

are all traveling at roughly the same speed, and so they all possess shapes given by weakly distorted homoclinic orbits. Thus, we can once more apply singular perturbation theory to determine the positions of the pulses. However, rather than a map of equilibrium pulse spacings, we now derive a set of coupled ODEs describing the evolution of the pulse's positions (McLaughlin & Scott 1978, Gorshkov & Ostrovsky 1982, Kawasaki & Ohta 1982, Couillet & Elphick 1989, Ohta & Mimura 1990).

To derive the asymptotic equations, we again introduce the traveling-wave coordinate $\zeta = x - ct$, where, since the pattern is now not steady, we set $c = c_0$. In this coordinate frame, the pulses move slowly under mutual, long-range interaction. To account for this we introduce the slow time-scale, $\tau = \varepsilon t$, upon which the pulse positions depend: $\zeta_k = \zeta_k(\tau)$. The asymptotic expansion then proceeds as in Section 3.1, the only difference being the replacement of the velocity correction term, $\varepsilon c_1 H_k$, with $\dot{\zeta}_k H_k$. The solvability condition is (e.g. Elphick et al 1990),

$$\dot{\zeta}_k = F(\Delta_k) + F(-\Delta_{k+1}), \quad (4.1)$$

which is the equation of motion of the k th pulse.

4.2 Sample Pattern Dynamics

An example of the pulse evolution predicted by Equation (4.1) is shown in Figure 12, which shows 12 isolated pulses adjusting from a set of arbitrary initial positions. The initial separations cover a moderate range and the pulses slowly lock into a steady pattern after proceeding through two distinct steps. The pulses first lock into three distinct, quasi-steady subgroups (Figure 12a). The subgroups then interact much more weakly; eventually they approach one another and merge into a single steady formation (Figure 12b). Evolution with two disjoint time and length scales arises from the exponential form of the interaction. This suggests that patterns of very many pulses evolve on a whole spectrum of scales, and that pulse dynamics creates spatio-temporal complexity (Elphick et al 1989).

A typical feature of evolution under the system (4.1) is gradual locking into a steady pattern. This highlights the importance of the equilibrium solutions discussed in the previous section. These equilibria only exist if $F(\Delta_k) + F(-\Delta_{k+1}) = \text{constant}$ has nontrivial solutions. In our current example this is guaranteed by the oscillatory tail of the homoclinic pulse, and the final pattern is one of a multitude of existing equilibria.

The example shown in Figure 12 follows the adjustments of an isolated group of 12 pulses. The steady pattern to which the pulses evolve is constrained by the termination of the pattern to the left and right. Different patterns result if the pulses are arrayed periodically (Elphick et al 1989),

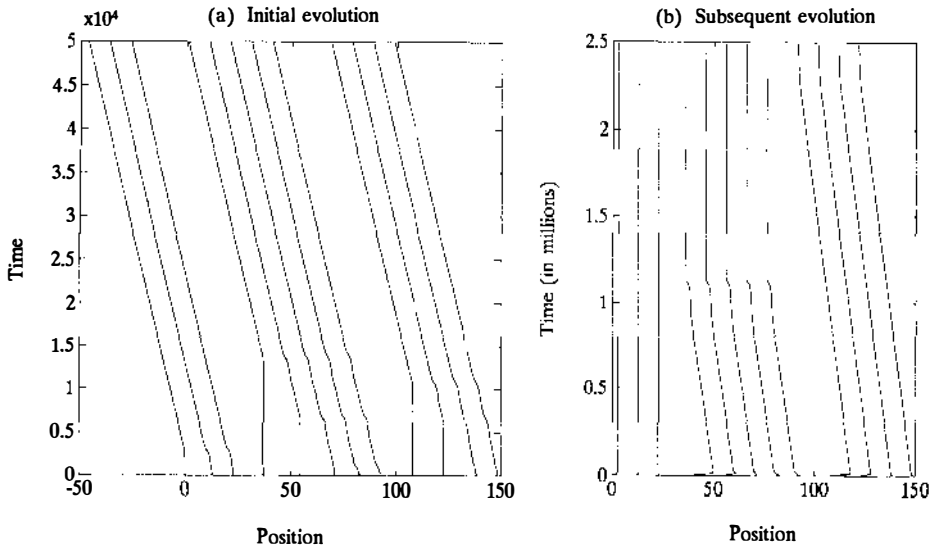


Figure 12 An example of the evolution of 12 pulses from arbitrary initial conditions computed using Equation (4.1). Initially, the pulses lock into 3 almost steady subgroups (a). These subgroups eventually coalesce into a single formation (b). In (b), a synchronized drift in the position of all of the pulses has been subtracted out. Parameter values are as in Figure 8.

or when they are sequentially generated at a fixed location (Elphick et al 1991b, Chang et al 1993a). Such constraints are equivalent to the boundary conditions imposed on the PDE.

4.3 *An Example of Frontal Dynamics*

An alternative kind of example, depicted in Figure 13, follows the evolution of an ensemble of kinks and antikinks for a real Ginzburg-Landau equation (Section 2.2; Elphick et al 1991c). The heteroclinic orbits corresponding to those kinks and antikinks monotonically decay into the fixed points. Consequently, the interaction potential represented by $F(\Delta)$ contains no minima and so the force between kinks and antikinks is always attractive. As a result, the kinks and antikinks drift slowly towards one another under mutual interaction. This creates slowly evolving metastable states. Inevitably, each state terminates in the catastrophic collision of a kink-antikink pair. This marks a violent event which cannot be captured by the asymptotic method. In Figure 13, the collisions have been crudely treated by assuming a smooth collision of the front positions.

The collision destroys one of the layers and a new metastable state then begins. The succession continues until as many annihilations as possible have occurred, all internal layers have vanished, and the asymptotic state

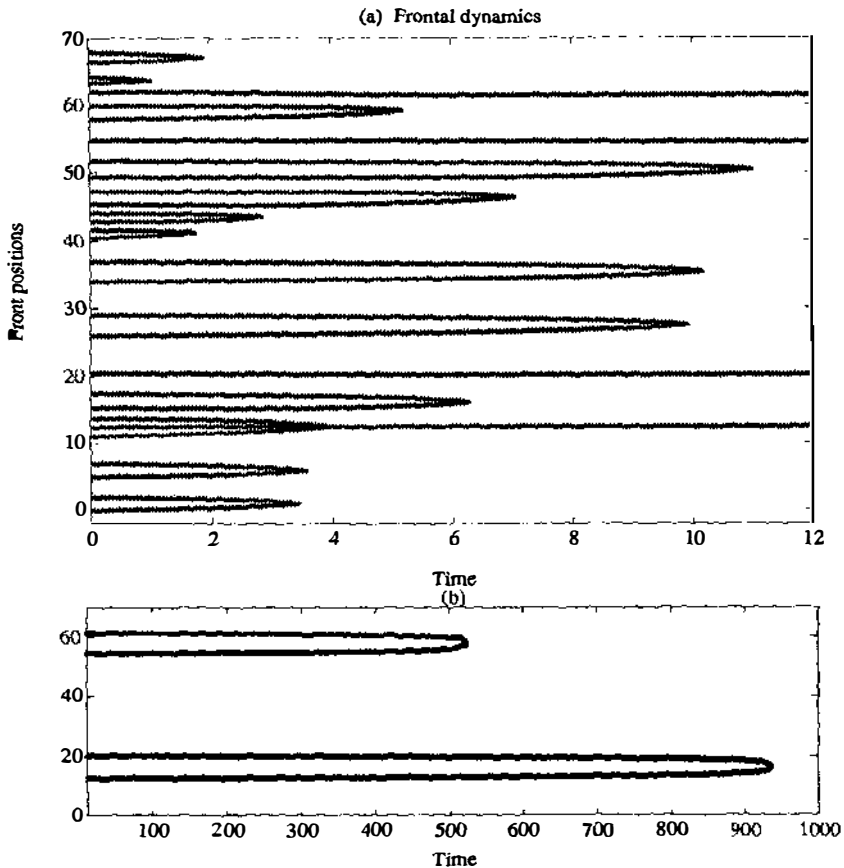


Figure 13 Frontal dynamics. (a) Positions of the fronts as they initially evolve and collide. (b) The eventual evolution and annihilation of the remaining four fronts after the initial phase. (Based on Elphick et al 1991c.)

is obtained. Further details of the problem are discussed by Carr & Pego (1989), Fusco & Hale (1989), and Nagai & Kawahara (1983).

The long-lived process illustrated in Figure 13 was derived for pattern evolution in a thermally relaxing medium (Elphick et al 1991c). Relaxation proceeds through fairly simple frontal dynamics which engender the run-down of complexity. The introduction of forcing can halt such a run-down. For example, Thual & Fauve (1988) and Malomed & Nepomnyashchy (1990) create kink-antikink bound states by introducing terms into the equation modeling weak dispersion. Elphick et al (1991c) generated com-

plicated steady patterns through a spatially periodic forcing. In either case, we add terms to the equations of motion (4.1) which change its steady solutions (the equilibrium patterns).

4.4 *Spacing Limitation and Some Setbacks*

We have used the PDE (2.1) as an example throughout this review to illustrate the theory of equilibrium states and dynamics of propagating pulses. This PDE is a particularly good example because the dynamics embodied in (4.1) fails completely to describe the solution if the pulse spacings become too large. This regime is precisely where one would expect the asymptotic theory to be most accurate, and the failure illustrates some of the pitfalls one could fall into by blindly applying the asymptotic machinery. A second common pitfall concerns additional invariances in the governing equation. These lead to extra free parameters in the theory that, in principle, one should fix by singular perturbation theory along with the pulse positions which represent translational invariance. For example, (2.1) also possesses Galilean invariance, although this does not appear to modify the dynamics unless the pattern is spatially extended. In contrast, the scale invariances of the nonlinear Schrödinger equation must be taken into account in any singular perturbation theory (Keener & McLaughlin 1977, Bretherton & Spiegel 1983); otherwise, the dynamics of the solitons are of an artificially low order.

To return to our example, the dynamical theory fails because a train of widely separated pulses contains extensive regions in which the amplitude of u is essentially vanishingly small. Linear theory, however, tells us that this *vacuum state* is unstable. In other words, if the pulse separations are too large, the remnant instability of the vacuum comes into play (Toh & Kawahara 1985, Chang et al 1993b). The instability takes the form of spatially unlocalized waves that we refer to as “radiation.” These are not taken into account by weak pulse interactions, and so (4.1) fails entirely to describe the dominant dynamics.

For large dispersion, the instabilities are subcritical and rapidly amplifying radiation modes destroy the pulse configuration. The outcome is the violent creation of new pulses (Toh & Kawahara 1985, Toh 1987, Elphick et al 1991a). The new state consists of a denser train of pulses, and radiation then damps out. This leaves an equilibrium state that can be described by the asymptotic theory.

Because radiative instabilities are critical at large spacings, the solutions shown in Figure 12 cannot be realised. Therefore, pulse dynamics alone cannot create spatio-temporal complexity on the liquid film. For alternative PDEs, however, like those describing excitable media (e.g. Ohta &

Mimura 1990) for which the vacuum state is stable, there are no limits on separation and spatio-temporal complexity can be obtained.

4.5 Radiation and Chaos in the KS Limit

For smaller dispersions, the bifurcation of separation-limiting radiation can be supercritical. Then we can find equilibrated states consisting of coexisting pulses and finite-amplitude radiation. One such state is shown in Figure 14. The radiation saturates at low amplitude, but it is sufficient to affect the tail of the pulse. This “shakes” the pulse just as the tails of neighboring pulses affect its position in a pattern. Forced oscillations of coherent structures have also been observed for fronts (Elezgaray & Arnedo 1991, Ikeda & Mimura 1993, Hagberg & Meron 1994).

A feature of the PDE (2.1) is that the separation-limiting Hopf bifurcations occur at smaller spacings at smaller dispersion. By the time dispersion disappears (the Kuramoto-Sivashinsky or KS limit), even moderately spaced pulses are unstable. Moreover, in this physical regime, the characteristic rates of amplitude decay away from the center of a pulse, σ and γ , become increasingly disparate. At $\mu = 0$, their ratio is 1/2, and pulses are too asymmetrical to be described by unmodified perturbation theory (Balmforth et al 1994). The limit is consequently not accessible to the present prescription of pulse dynamics.

The inability of our theory to describe pulse dynamics in the KS limit is

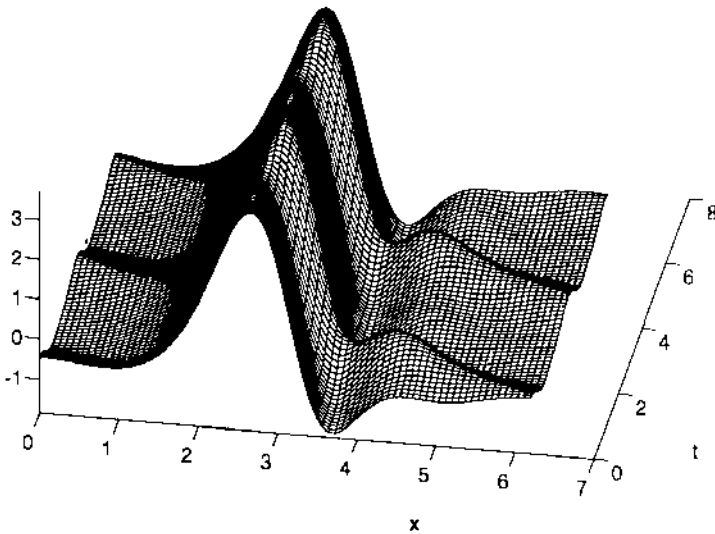


Figure 14 An illustration of a pulse with a supercritically saturated, radiative instability. Shown is a space-time surface plot, computed for periodic boundary conditions and $\mu = 0.4$.

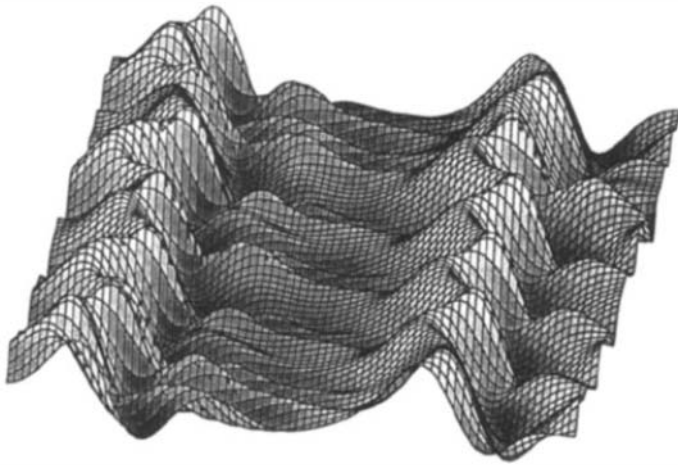


Figure 15 A two-pulse chaotic state. Shown is a space-time surface plot, computed for periodic boundary conditions and $\mu = 0.1$. Time recedes into the page; space increases to the right. (Based on Elphick et al 1991a.)

particularly unsatisfying because here one typically finds spatio-temporal chaos (e.g. Hyman et al 1986, Pumir 1985); incoherent interactions between pulses and a bath of radiation may be responsible for producing such a state (Toh 1987, Elphick et al 1991a). Figure 15 shows a chaotic state arising from a two-pulse equilibrium state subject to three radiative instabilities.

The bifurcation structure of the Kuramoto-Sivashinsky equation and its chaotic states are varied and complicated (Hyman et al 1986). Our view of KS chaos as interacting pulses and radiation is excessively simplistic. For example, it is not always possible to unambiguously distinguish moving pulses from the radiation. We also cannot ignore the fact that pulses are occasionally destroyed and nucleated as a result of hard collision and violent instability (Sekimoto et al 1987, Toh 1987). Moreover, in addition to pulses like that shown in Figure 5, there are other, multiply peaked pulses and shock solutions (Balmforth et al 1994, Chang et al 1993b, Hooper & Grimshaw 1988, Kent & Elgin 1992, Michelson 1986) that may also play a role in the full dynamics.

5. SOME LOOSE ENDS AND OUTLOOK

In this final section we mention some related issues to the main discussion. Our survey is not meant to be a complete one, and we only summarize some topics of particular interest. Firstly, we address some important

issues of stability that might arise in attempting to apply the asymptotic machinery in any practical situation. Then, we establish the connection between the theory outlined here and some other related techniques. Finally, we remark on the relevance of the theory to the real world.

5.1 *Issues of Stability*

In discussing either interacting pulses or dynamics near homoclinic orbits, we have implicitly made an assumption regarding the stability of these special types of solutions. One circumstance in which this assumption breaks down is radiative instability, but there are other cases.

In the context of ODEs, for nearly-homoclinic dynamics, there is an intrinsic notion that trajectories in phase space hug the homoclinic orbit as they traverse the main peaks of the pulses. Then, in the geometrical vision of Shil'nikov theory, the trajectory does not deviate too wildly from $H(\xi)$ as it circulates outside of the region \mathcal{C} shown in Figure 6. In singular perturbation theory, there is no such assumption, but there is also no guarantee that the approximate solutions characterized by the spacing map possess any degree of stability whatsoever. In other words, for either visualization, in order for the homoclinic solutions to be interesting, they must, in some sense, possess a degree of both stability and instability. Without the former, no trajectory ever remains nearly homoclinic, but without the latter, the solutions are not chaotic.

For three-dimensional homoclinics, trajectories often remain near $H(\xi)$ when that orbit possesses a large and negative Floquet exponent. If the flow in phase space contracts volumes sufficiently strongly (i.e. if μ is sufficiently large), one exponent is likely to be of this form. For chaos, the other nontrivial Floquet exponent should be small but positive, and Shil'nikov theory tells us that this transpires for $\delta \lesssim 1$.

Stability of a pulse in the PDE is not the same as the stability of $H(\xi)$ in the phase space of the associated dynamical system. For pulse solutions of a PDE, the question of stability constitutes a more delicate issue. Radiative instability highlights the possibility that the pulse may be a stable homoclinic orbit in the ODE, but it does not evolve accordingly. In fact, there is no reason to suppose that, in general, the pulse train is remotely stable. In Equation (2.1), the supercritical bifurcation of the periodic vacuum state is partly the reason why the pulse solutions are stable at short spacing.

Pulse stability can be rigorously established in some circumstances. In more general situations, numerical stability analysis (e.g. Toh & Kawahara 1985, Chang et al 1993b, Elphick et al 1991a) or variants of the Nyquist method (e.g. Evans & Feroe 1975, Swinton & Elgin 1990) can be used. For the Fitz-Hugh/Nagumo equation it has been established that pulses

are often stable. Interestingly, these correspond to strongly unstable homoclinic orbits, in contrast to the solitary waves of Equation (2.1). Therefore, even though the nerve equation generates spatially irregular patterns of pulses (Elphick et al 1991b), one cannot find corresponding strange attractors as solutions to the associated ODE.

5.2 *Hamiltonian Dynamics and Melnikov Theory*

In this review we have been concerned primarily with dissipative systems. Equally well, however, we could have specialized to Hamiltonian homoclinic dynamics. The parallel of Shil'nikov theory which is typically used for Hamiltonian systems is Melnikov theory. Like Shil'nikov theory, this is a geometrically based approach to uncovering the dynamics in the vicinity of a broken homoclinic connection (Melnikov 1963). The ideas are most simply illustrated for a Hamiltonian system with a single degree of freedom under periodic perturbation (e.g. Drazin 1993). If the unperturbed system admits a homoclinic solution, then under perturbation, the connection of the stable and unstable manifolds is broken; Melnikov theory amounts to determining the distance between the two manifolds.

The key ingredient in Melnikov's analysis is an integral $M(t_0)$ which measures the splitting of the manifolds (t_0 parameterizes the position along the unperturbed homoclinic orbit). This integral is commonly called Melnikov's function. If, for some t_0 , it vanishes, then we infer that the manifolds cross. Because the perturbation is also periodic, it further implies that $M(t_0)$ is likewise periodic, and so the manifolds intersect one another an infinite number of times. The entangling of the manifolds (a "homoclinic tangle") signifies the existence of chaotic orbits, and is the analogue of Shil'nikov's theorem.

Melnikov theory is rather elegantly formulated in the framework of Hamiltonian dynamics. But it need not be couched in those terms (Chow et al 1980). In fact, as pointed out by Coulet & Elphick (1987), the Melnikov method for dissipative systems is essentially the same as singular perturbation theory. The Melnikov function in that context is simply the integral solvability condition; the requirement that it vanish ensures bounded solutions in the asymptotic calculation, which is equivalent to saying that the manifolds entangle. But, just as Shil'nikov theory provides more geometrical information regarding the dynamics around the homoclinic orbits than the spacing map, so too does Melnikov theory.

5.3 *Painlevé Analysis and Pole Expansion*

Our approach to the problem of pulse dynamics has been founded on the idea that solitary waves correspond to homoclinic orbits of the dynamical system associated to the governing PDE. Save for some special cases, these

orbits need to be determined numerically, at least for most dissipative systems. This is not, however, the only approach one can take to the problem. Exact, analytical solitary solutions can also be furnished by Painlevé analysis (Weiss et al 1983). Though intimately connected with integrable systems, the Painlevé method occasionally works for dissipative systems. The heteroclinic solution of the KS equation which is pictured in Figure 5 can be uncovered in this fashion (Conte & Musette 1989), as can several frontal solutions of Equation (2.1) at particular values of the dispersion parameter (Kudryashov 1990). The trouble with uncovering analytical solutions in this way is that it is rarely possible, and certainly gives no indication of the wealth of solutions possible. Yet when the analysis furnishes an analytical solution, it can be very useful.

A somewhat related method for pulse dynamics is pole expansion. This was first applied to derive soliton solutions for the KdV equation and some of its relatives (Kruskal 1975, Airault et al 1977). Unlike approximation by homoclinic orbits, the method centers around the idea that, by choosing an appropriate selection of rational functions, we can obtain exact nonlinear solutions. This amounts to finding a finite set of movable singular or pole solutions that solve the PDE exactly, provided their positions satisfy certain ODEs. Once again, this method only works under special circumstances, and is at least partially connected to integrability. But unlike singular perturbation theory and Equation (4.1), the dynamical equations that one extracts with pole expansion are exact nonlinear evolution equations for the pole positions, which may or may not resemble individual pulses. In addition to the KdV equation, this technique has been employed to find solutions of the dissipative Benjamin-Ono equation (Meiss 1980, Birnir 1986, Qian et al 1989) and a variation of the Boussinesq equation (Qian & Spiegel 1994).

5.4 *Relevance to the Real World*

What we have described in this review is a theory of the dynamics of homoclinic orbits in an ODE, and of pulses in a PDE. In the real world, most systems have too many degrees of freedom to be described by a simple theory of this kind. For systems describable by ODEs, this is the main reason why there are very few examples of experimental spacing maps like those pictured here, even when the object under study bursts sporadically and would appear nearly homoclinic [laser dynamics has something of the flavor of homoclinic theory (Arrechi et al 1993, Papoff et al 1991)]. One important difference is that there can be intrinsic noise in experimental systems. This restricts the accessibility of phase space near the origin, with critical repercussions on the spacing map (Hughes & Proctor 1990, Stone & Holmes 1991, Arrechi et al 1993).

In asymptotic theory, noise can be added perturbatively. This influences the solvability condition in a similar fashion to the perturbations of the Ginzburg-Landau equation mentioned in Section 4.3. The equations of motion become

$$\dot{\zeta}_k = F(\Delta_k) + F(-\Delta_{k+1}) + g_k, \quad (5.1)$$

where g_k depends on the pulse positions for deterministic perturbations, and is a stochastic variable in the case of noise. Accordingly, deterministic perturbations intrinsically change the pattern map for the equilibrium pulse trains. Noise, on the other hand, stochastically drives the pulses like pollen grains forced into Brownian motion.

As regards experimental observations of pulse dynamics in spatio-temporal systems, the situation is again difficult to compare with theory. Solitary waves on fluid films are subject to secondary instabilities which typically wreck the possibility of recording persistent one-dimensional interaction (Chang et al 1993a). In spite of this drawback, some of the results of Liu & Gollub (1994) suggest that experimental analogues might be found for fluid films. In binary fluid convection, only a small number of pulses invariably emerge in the system, and it does not seem currently possible to describe these with simple PDEs.

The theory described here is most useful in pointing to a way of completely describing spatio-temporal complexity in a simple system. Though real systems are generally substantially more complicated, the understanding gained in such a simple situation will hopefully provide invaluable insights into more physical cases. In higher dimension, things only become worse and we open Pandora's box. Geometrically alone, pulses can take shapes of all kinds, from disks and spheroids to spirals and scrolls. Weak interaction theory could provide the interaction potentials necessary for the dynamics of these coherent structures, if they could be regarded as point particles. Then, many-body dynamics could be attempted. But even in one dimension, we have seen that this approach often is not enough.

ACKNOWLEDGMENTS

I thank L. N. Howard, G. R. Ierley, P. J. Morrison, E. A. Spiegel, and C. Tresser for comments, conversations, and criticisms. This work was supported by the Air Force Office of Scientific Research under Grant No. AFOSR89-0012.

Any *Annual Review* chapter, as well as any article cited in an *Annual Review* chapter, may be purchased from the *Annual Reviews* Preprints and Reprints service.
1-800-347-8007; 415-259-5017; email: arpr@class.org

Literature Cited

- Ablowitz MJ, Segur H. 1981. *Solitons and the Inverse Scattering Transform*. Philadelphia: SIAM
- Airault H, McKean HP, Moser JE. 1977. Rational and elliptic solutions of the Korteweg-de Vries equation and a related many-body problem. *Comm. Pure Appl. Math.* 30: 95–148
- Alekseenko SV, Nakoryakov VY, Pokusaev BG. 1985. Wave formation on a vertically falling liquid film. *AIChE J.* 31: 1446–60
- Anderson KE, Behringer RP. 1990. Long timescales in traveling-wave convection patterns. *Phys. Lett. A* 145: 323–28
- Argoul F, Arneodo A, Richetti P. 1987. Experimental evidence for homoclinic chaos in the Belousov-Zhabotinskii reaction. *Phys. Lett.* 120A: 269–75
- Arneodo A, Coulet PH, Spiegel EA. 1985a. Dynamics of triple convection. *Geophys. Astrophys. Fluid Dyn.* 31: 1–48
- Arneodo A, Coulet PH, Spiegel EA, Tresser C. 1985b. Asymptotic chaos. *Physica D* 14: 327–47
- Arrechi FT, Lapucci A, Meucci R. 1993. Poincaré versus Boltzmann in Shil'nikov phenomena. *Physica D* 62: 186–91
- Balmforth NJ, Ierley GR, Spiegel EA. 1994. Chaotic pulse trains. *SIAM J. Appl. Math.* 54: 1291–334
- Benney DJ. 1966. Long waves on liquid films. *J. Math. Phys.* 45: 150–55
- Ben-Jacob E, Brand H, Dee G, Kramer L, Langer JS. 1985. Pattern propagation in nonlinear dissipative systems. *Physica D* 14: 348–64
- Bensimon D, Kolodner P, Surko CM, Williams H, Croquette V. 1990. Competing and co-existing dynamical states of travelling-wave convection in an annulus. *J. Fluid Mech.* 217: 441–67
- Birnir B. 1986. Chaotic perturbations of KdV. 1. Rational solutions. *Physica D* 19: 238–54
- Bretherton CS, Spiegel EA. 1983. Intermittency through modulational instability. *Phys. Lett.* 96A: 152–56
- Carr J, Pego RL. 1989. Meta-stable patterns in solutions of $u_t = \varepsilon^2 u_x x - f(u)$. *Comm. Pure Appl. Math.* 17: 523–76
- Champneys AR, Toland JF. 1993. Bifurcation of a plethora of multi-modal homoclinic orbits for autonomous Hamiltonian systems. *Nonlinearity* 6: 655–721
- Chang H-C. 1994. Wave evolution on a falling film. *Annu. Rev. Fluid Mech.* 26: 103–36
- Chang H-C, Demekhim EA, Kopelevich DI. 1993a. Nonlinear evolution of waves on a vertically falling film. *J. Fluid Mech.* 250: 433–80
- Chang H-C, Demekhim EA, Kopelevich DI. 1993b. Laminarizing effects of dispersion in an active-dissipative nonlinear medium. *Physica D* 63: 299–320
- Chaté H. 1994. Disordered regimes of the one-dimensional complex Ginzburg-Landau equation. *Nonlinearity* 7: 185–204
- Chow SN, Hale JK, Mallet-Paret J. 1980. An example of bifurcation to homoclinic orbits. *J. Diff. Eq.* 37: 351–73
- Conte R, Musette M. 1989. Painlevé analysis and Bäcklund transformation in the Kuramoto-Sivashinsky equation. *J. Phys. A* 22: 169–77
- Coulet P, Elphick C. 1987. Topological defect dynamics and Melnikov's theory. *Phys. Lett.* 121A: 233–36
- Coulet P, Elphick C. 1989. Rhythms and pattern transitions. *Phys. Scr.* 40: 398–408.
- Drazin PG. 1993. *Nonlinear Systems*. Cambridge: Cambridge Univ. Press
- Elezgaray J, Arneodo A. 1991. Modelling reaction-diffusion pattern formation in the Couette flow reactor. *J. Chem. Phys.* 95: 323–50
- Elphick C, Ierley GR, Regev O, Spiegel EA. 1991a. Interacting localized structures with Galilean invariance. *Phys. Rev. A* 44: 1110–22
- Elphick C, Meron E, Rinzel J, Spiegel EA. 1991b. Impulse patterning and relaxational propagation in excitable media. *J. Theor. Biol.* 146: 249–68
- Elphick C, Meron E, Spiegel EA. 1989. Spatio-temporal complexity in travelling patterns. *Phys. Rev. Lett.* 61: 496–99
- Elphick C, Meron E, Spiegel EA. 1990. Patterns of propagating pulses. *SIAM J. Appl. Math.* 50: 490–503
- Elphick C, Regev O, Spiegel EA. 1991c. Complexity from thermal instability. *Mon. Not. R. Astron. Soc.* 250: 617–28
- Evans JW, Feroe JA. 1977. Local stability theory of the nerve impulse. *Math. Biosci.* 37: 23–50
- Flesselles J-M, Simon AJ, Libchaber AJ. 1991. Dynamics of one-dimensional interfaces: an experimentalist's view. *Adv. Phys.* 40: 1–51
- Fowler AC, Sparrow CT. 1991. Bifocal homoclinic orbits in four dimensions. *Nonlinearity* 4: 1159–82
- Fusco G, Hale JK. 1989. Slow-motion manifolds, dormant instability, and singular perturbations. *J. Dyn. Diff. Eq.* 1: 75–94
- Gaspard P, Wang X-L. 1987. Homoclinic orbits and mixed-mode oscillations in far-from-equilibrium systems. *J. Stat. Phys.* 48: 151–91
- Glendinning P. 1984. Bifurcations near

- homoclinic orbits with symmetry. *Phys. Lett.* 103A: 163–66
- Glendinning P, Sparrow CT. 1984. Local and global behavior near homoclinic orbits. *J. Stat. Phys.* 35: 645–96
- Glendinning P, Tresser C. 1985. Heteroclinic loops leading to hyperchaos. *J. Phys. (Paris)* 46: L347–52
- Gol'dshtik MA, Shtern VN. 1981. Theory of structural turbulence. *Sov. Phys. Dokl.* 257: 1319–22
- Gorshkov KA, Ostrovsky LA. 1981. Interactions of solitons in non-integrable systems: direct perturbation method and applications. *Physica D* 3: 424–38
- Hagberg A, Meron E. 1994. Pattern formation in non-gradient reaction-diffusion systems: the effects of front bifurcations. *Nonlinearity* 7: 805–36
- Hirschberg P, Knobloch E. 1993. Shil'nikov-Hopf bifurcation. *Physica D* 62: 202–16
- Hooper AP, Grimshaw R. 1988. Travelling wave solutions of the Kuramoto-Sivashinsky equation. *Wave Motion* 10: 405–20
- Howard LN, Krishnamurti R. 1986. Large-scale flow in turbulent convection: a mathematical model. *J. Fluid Mech.* 170: 385–410
- Hughes DW, Proctor MRE. 1990. A low-order model of the shear instability of convection: chaos and the effect of noise. *Nonlinearity* 3: 127–54
- Hyman JH, Nicolenko B, Zaleski S. 1986. Order and complexity in the Kuramoto-Sivashinsky model of weakly turbulent interfaces. *Physica D* 23: 265–92
- Ikeda T, Mimura M. 1993. An interfacial approach to regional segregation of two competing species mediated by a predator. *J. Math. Biol.* 31: 215–40
- Janiaud B, Pumir A, Bensimon D, Croquette V, Richter H, Kramer L. 1992. The Eckhaus instability for travelling waves. *Physica D* 55: 269–86
- Joets A, Ribotta R. 1988. Localized, time-dependent state in the convection of a nematic liquid crystal. *Phys. Rev. Lett.* 60: 2164–67
- Kath WL, Knessl C, Matkowsky BJ. 1987. A variational approach to nonlinear singularly perturbed boundary-value problems. *Stud. Appl. Math.* 77: 61–88
- Kawahara T, Toh S. 1987. Pulse interactions in an unstable dissipative-dispersive nonlinear system. *Phys. Fluids* 31: 2103–11
- Kawasaki K, Ohta T. 1982. Kink dynamics in one-dimensional nonlinear systems. *Physica A* 116: 573–93
- Keener JP, McLaughlin DW. 1977. Solitons under perturbations. *Phys. Rev. A* 16: 777–90
- Kent P, Elgin J. 1992. Travelling-wave solutions of the Kuramoto-Sivashinsky equation: period-multiplying bifurcations. *Nonlinearity* 4: 899–920
- Kivshar YS, Malomed BA. 1989. Dynamics of solitons in nearly integrable systems. *Rev. Mod. Phys.* 61: 763–916
- Knobloch E, Weiss N. 1983. Bifurcations in a model of magnetoconvection. *Physica D* 9: 379–407
- Kolodner P. 1991a. Drift, shape, and intrinsic destabilization of pulses of travelling-wave convection. *Phys. Rev. A* 44: 6448–65
- Kolodner P. 1991b. Collisions between pulses of travelling-wave convection. *Phys. Rev. A* 44: 6466–79
- Kolodner P, Glazier JA, Williams H. 1990. Dispersive chaos in one-dimensional travelling-wave convection. *Phys. Rev. Lett.* 65: 1579–82
- Kopell N, Howard LN. 1981. Target patterns and horse shoes from a perturbed central-force problem: some temporally periodic solutions to reaction-diffusion equations. *Stud. Appl. Math.* 64: 1–56
- Kruskal MD. 1975. In *Nonlinear Wave Motion*, ed. AC Newell, 15: 61–83. Providence, RI: Am. Math. Soc.
- Kudryashov NA. 1990. Exact solutions of the generalized Kuramoto-Sivashinsky equation. *Phys. Lett.* 147A: 287–91
- Kuramoto Y. 1984. *Chemical Oscillations, Waves and Turbulence*. Berlin: Springer-Verlag
- Liu J, Gollub JP. 1994. Solitary wave dynamics of film flows. *Phys. Fluid* 6: 1702–12
- Liu J, Paul JD, Gollub JP. 1993. Measurements of the primary instabilities of film flows. *J. Fluid Mech.* 250: 69–101
- Malomed B, Nepomnyashchy AA. 1990. Kinks and solitons in the generalized Ginzburg-Landau equation. *Phys. Rev. A* 42: 6009–14
- Manneville P. 1990. *Dissipative Structures and Weak Turbulence*. New York: Academic
- McLaughlin DW, Scott AC. 1978. Perturbation analysis of fluxon dynamics. *Phys. Rev. A* 18: 1652–80
- Meiss JD. 1980. Rational solutions to some partial differential equations. In *Geophysical Fluid Dynamics*, WHOI 80-53, pp. 155–64. Woods Hole, MA: Woods Hole Oceanogr. Inst.
- Melnikov VK. 1963. On the stability of the centre for time periodic perturbations. *Trans. Moscow Math.* 12: 1–57
- Michelson D. 1986. Steady solutions of the Kuramoto-Sivashinsky equation. *Physica D* 19: 89–111
- Moses E, Fineberg F, Steinberg V. 1987. Multistability and confined travelling-

- wave patterns in a convecting binary mixture. *Phys. Rev. A* 35: 2757–60
- Nagai T, Kawasaki K. 1983. Molecular dynamics of interacting kinks I. *Physica A* 120: 387–99
- Niemela JJ, Ahlers G, Cannell DS. 1990. Localized traveling-wave states in binary-fluid convection. *Phys. Rev. Lett.* 64: 1365–68
- Nozaki K, Bekki N. 1986. Low-dimensional chaos in a driven damped nonlinear Schrödinger equation. *Physica D* 21: 381–93
- Ohta T, Mimura M. 1990. Pattern dynamics in excitable media. In *Formation, Dynamics and Statistics of Patterns*, ed. K Kawasaki, M Suzuki, A Onuki, Vol. 1, pp. 55–112. Singapore: World Scientific
- Papoff F, Fioretti A, Arimondo E. 1991. Return maps for intensity and time in a homoclinic-chaos model applied to a laser with a saturable absorber. *Phys. Rev. A* 44: 4369–651
- Pumir A. 1985. Statistical properties of an equation describing fluid interfaces. *J. Phys. (Paris)* 46: 511–22
- Qian S, Lee YC, Chen HH. 1989. A study of nonlinear dynamical models of plasma turbulence. *Phys. Fluids B* 1: 87–98
- Qian ZS, Spiegel EA. 1994. Autogravity waves in a polytropic layer. *Geophys. Astrophys. Fluid Dyn.* 74: 225–43
- Sekimoto K, Kawasaki K, Ohta H. 1987. Aspects of nucleation and drift processes in a one-dimensional model. *J. Stat. Phys.* 48: 1213–41
- Shil'nikov LP. 1965. A case of the existence of a countable number of periodic motions. *Sov. Math. Dokl.* 6: 163–66
- Shil'nikov LP. 1970. A contribution to the problem of the structure of an extended neighborhood of a rough equilibrium state of saddle-focus type. *Math. USSR Sb.* 10: 91–102
- Shraiman B, Pumir A, van Saarloos W, Hohenberg PC, Chaté H, Holen M. 1992. Spatiotemporal chaos in the one-dimensional complex Ginzburg-Landau equation. *Physica D* 57: 241–48
- Sparrow C. 1982. *The Lorenz Equations: Bifurcations, Chaos and Strange Attractors*. New York: Springer-Verlag
- Stone E, Holmes P. 1991. Unstable fixed points, heteroclinic cycles and exponential tails in turbulence production. *Phys. Lett.* 155A: 29–42
- Swinton J, Elgin J. 1990. Stability of travelling pulse solutions to a laser equation. *Phys. Lett.* 145A: 428–33
- Thual O, Fauve S. 1988. Localized structures generated by subcritical instabilities. *J. Phys. (Paris)* 49: 1829–33
- Tilley BS, Davis SH, Bankoff SG. 1992. Stability of stratified fluids in an inclined channel. *Bull. Am. Phys. Soc.* 37: 1718
- Toh S. 1987. Statistical model with localized structures describing the spatio-temporal chaos of Kuramoto-Sivashinsky equation. *J. Phys. Soc. Jpn.* 56: 949–62
- Toh S, Kawahara T. 1985. On the stability of soliton-like pulses in a nonlinear dispersive system with instability and dissipation. *J. Phys. Soc. Jpn.* 54: 1257–69
- Tresser C. 1981. *Modèles simples de transition vers la turbulence*. PhD thesis. Univ. Nice, France
- Tresser C. 1984a. About some theorems of Shil'nikov. *Ann. Inst. H. Poincaré* 40: 441–61
- Tresser C. 1984b. Homoclinic orbits for flows in R^3 . *J. Phys. (Paris)* 45: 837–41
- van Saarloos W. 1989. Front propagation into unstable states: marginal stability as a dynamical mechanism for velocity selection. *Phys. Rev. A* 37: 211–29
- van Saarloos W, Hohenberg P. 1993. Fronts, pulses, sources and sinks in generalized Ginzburg-Landau equations. *Physica D* 56: 303–47
- Ward MJ. 1992. Eliminating indeterminacy in singularly perturbed boundary value problems with translational invariant potentials. *Stud. Appl. Math.* 87: 95–134
- Ward MJ. 1994. Metastable patterns, layer collapses, and coarsening for a one-dimensional Ginzburg-Landau equation. *Stud. Appl. Math.* 91: 51–93
- Weiss J, Tabor M, Carnevale G. 1983. The Painlevé property for partial differential equations. *J. Math. Phys.* 24: 522–26
- Wu J, Keolian R, Rudnick I. 1984. Observation of a nonpropagating hydrodynamic soliton. *Phys. Rev. Lett.* 52: 1411–24